Excitation and decay of light hypernuclei

C.A. Bertulani

TEXAS A&M UNIVERSITY
COMMERCE

STRONG 2020

This project has received funding from the European Union's Horizon 2020 research and innovation programme under grant agreement No 824093

From laboratory experiments to neutron stars

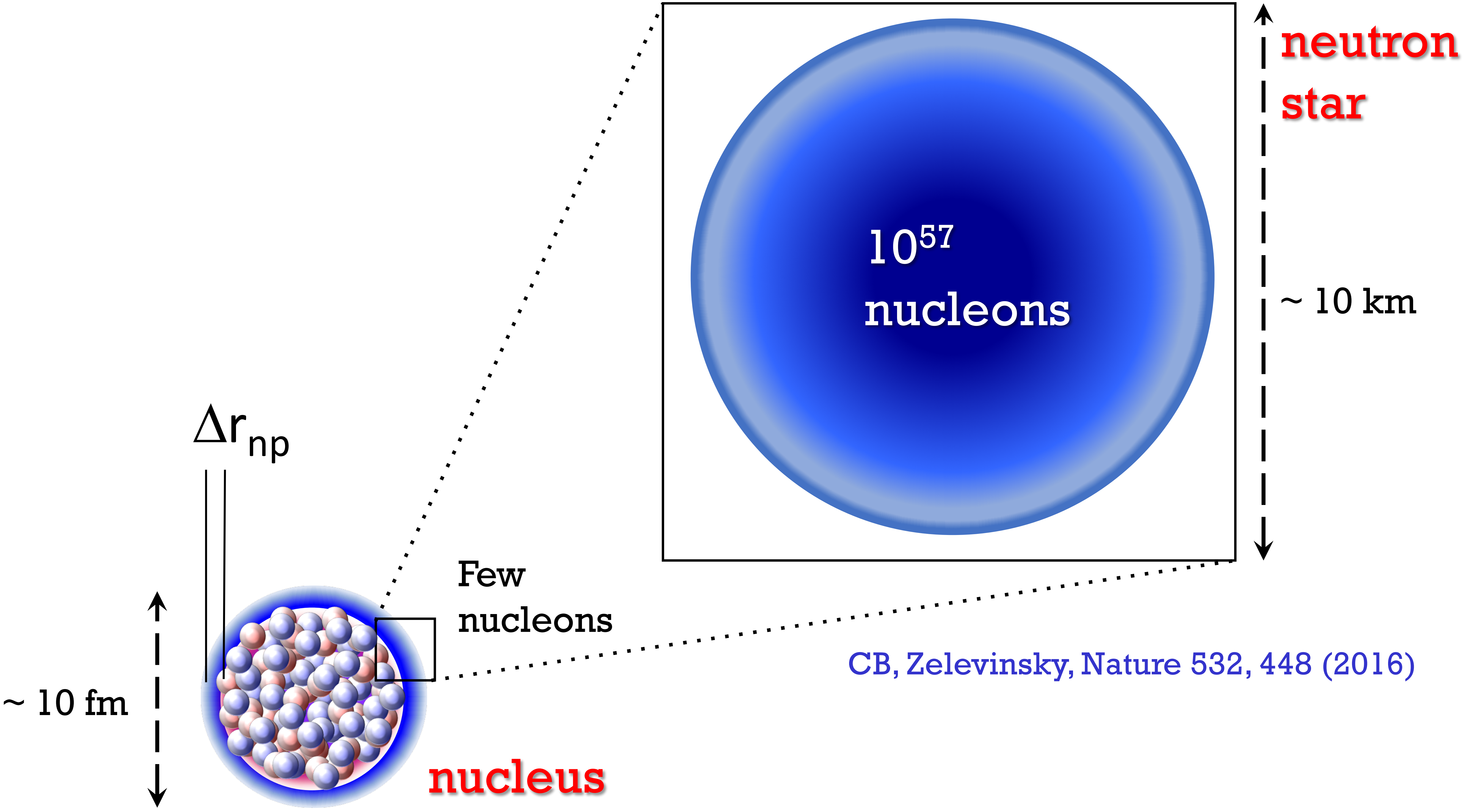

CB, Zelevinsky, Nature 532, 448 (2016)

From bones to dinosaurs

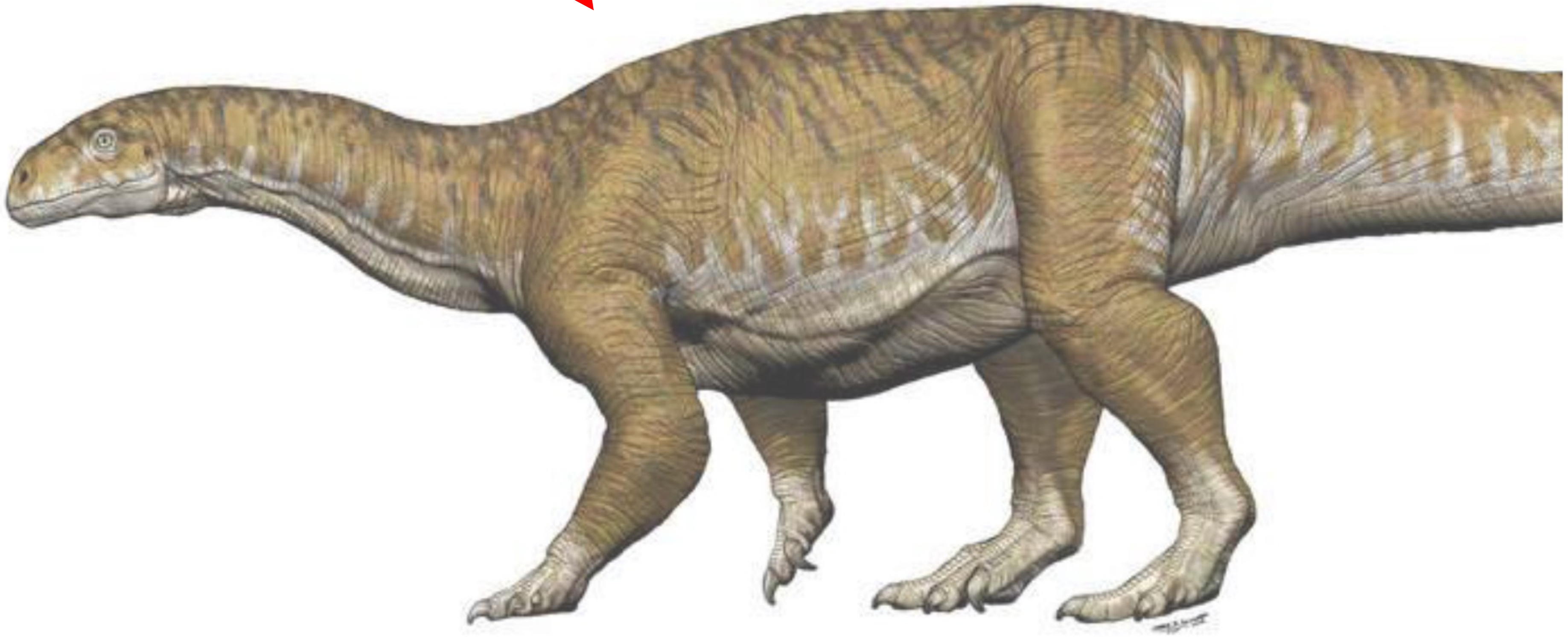

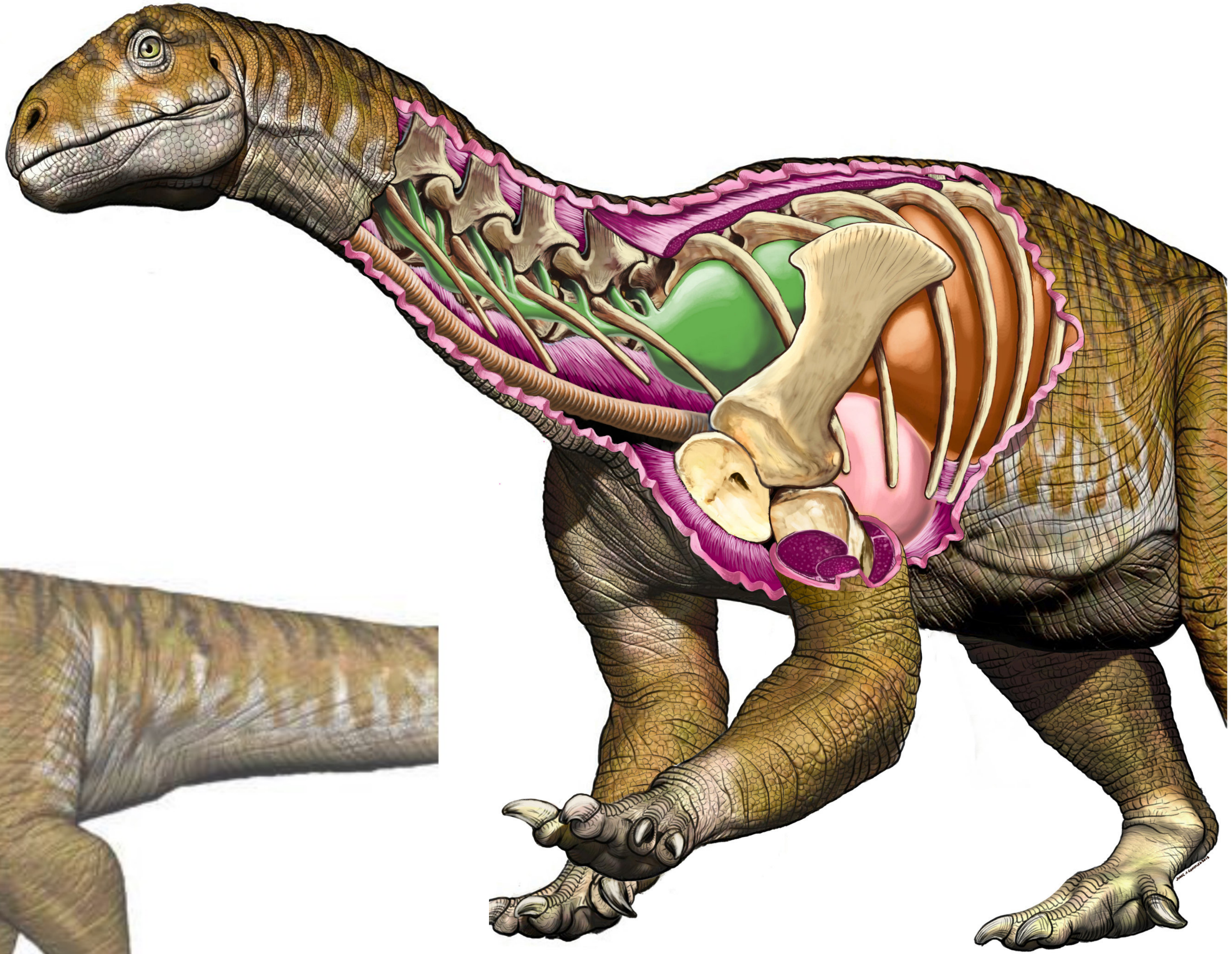

Credit: Nature Ecology & Evolution (2018)

Reconstruction of Ingentia prima from the Late Triassic (205- 210Ma) of Argentina. Total length 8-10 me…

Neutron stars

$$\frac{dP}{dr} = -\frac{G\rho(r)M(r)}{r^2}\left[1+\frac{P(r)}{\rho(r)}\right]\left[1+\frac{4\pi r^3 P(r)}{M(r)}\right]\left[1-\frac{2GM(r)}{r}\right]^{-1}$$

$$\frac{dM}{dr} = 4\pi r^2 \rho(r)$$

Tolman-Oppenheimer-Volkoff

EOS

$$p[\rho] = \rho^2 \frac{d}{d\rho}\left(\frac{E}{A}[\rho]\right)$$

$$\frac{E}{A}[\rho] = \frac{E}{A}[\rho_0] + \frac{1}{18}K_\infty\left(\frac{\rho-\rho_0}{\rho_0}\right)^2 + \cdots$$

$$K_\infty = 9\rho^2 \left.\frac{d^2[E/A]}{d\rho^2}\right|_{\rho_0}$$

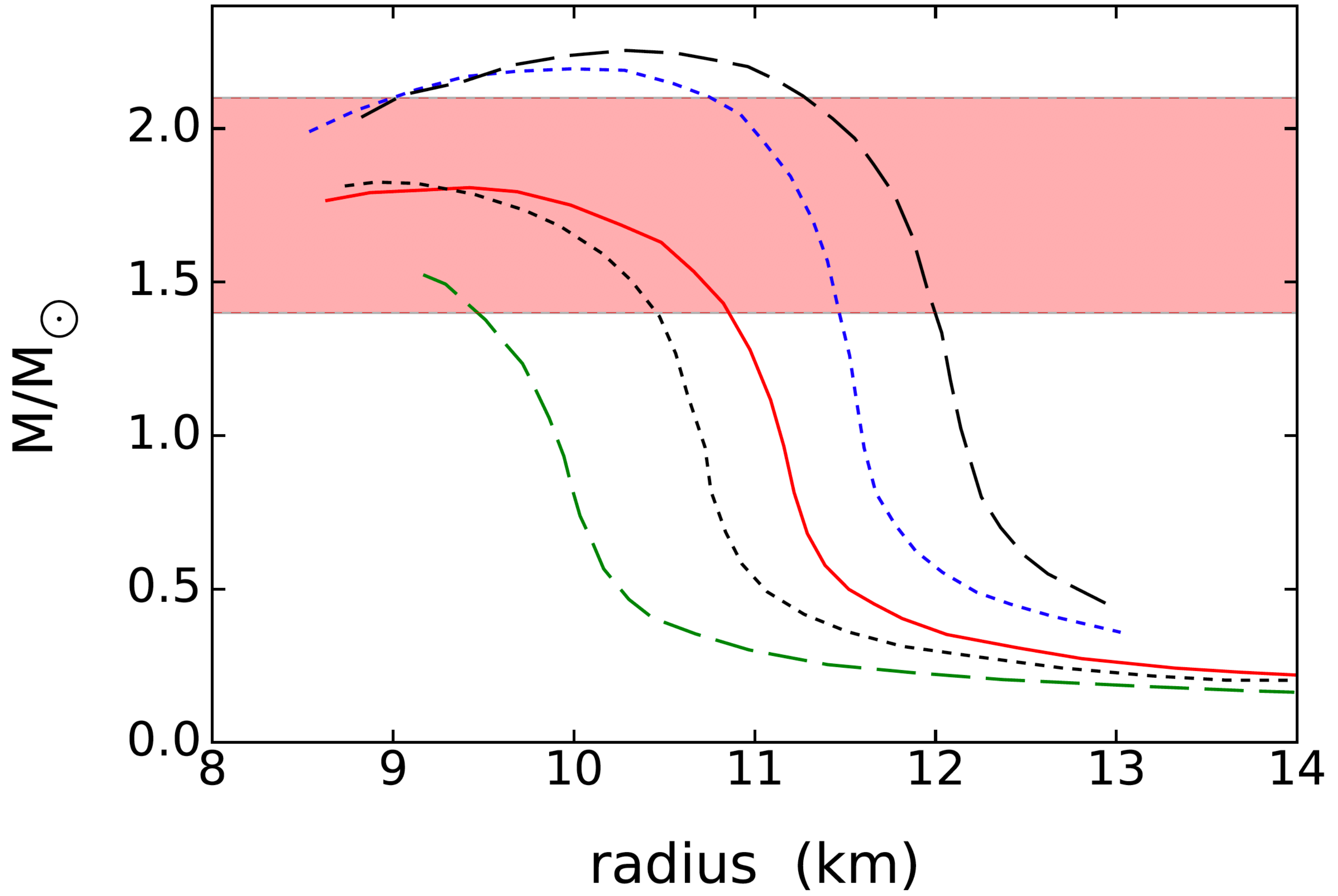

EOS + symmetry energy

$$\frac{E}{A}[\rho] = \frac{E}{A}[\rho_0] + \frac{1}{18} K_\infty \left(\frac{\rho - \rho_0}{\rho_0} \right)^2 + S \left(\frac{\rho_n - \rho_p}{\rho} \right)^2 + \cdots$$

$$S = \frac{1}{2} \frac{\partial^2 (E/A)}{\partial \delta^2} \bigg|_{\delta=0} = J + Lx + \frac{1}{2} K_{sym} x^2 + O(x^3),$$

$$L = 3\rho_0 \frac{dS(\rho)}{d\rho} \bigg|_{\rho_0}, \quad \delta = \frac{\rho_n - \rho_p}{\rho}, \quad x = \frac{(\rho - \rho_0)}{3\rho_0}$$

For $\rho \sim \rho_0$ and $\delta \sim 1 \Rightarrow p = \frac{L\rho_0}{3}$

Skyrme	ρ_0	E_0	K_∞	J	L	K_{sym}
SLy5	0.161	-15.99	229.92	32.01	48.15	-112.76
SkM*	0.160	-15.77	216.61	30.03	45.78	-155.94
Skxs20	0.162	-15.81	201.95	35.50	67.06	-122.31

L crucial for neutron matter

EOS of neutron stars

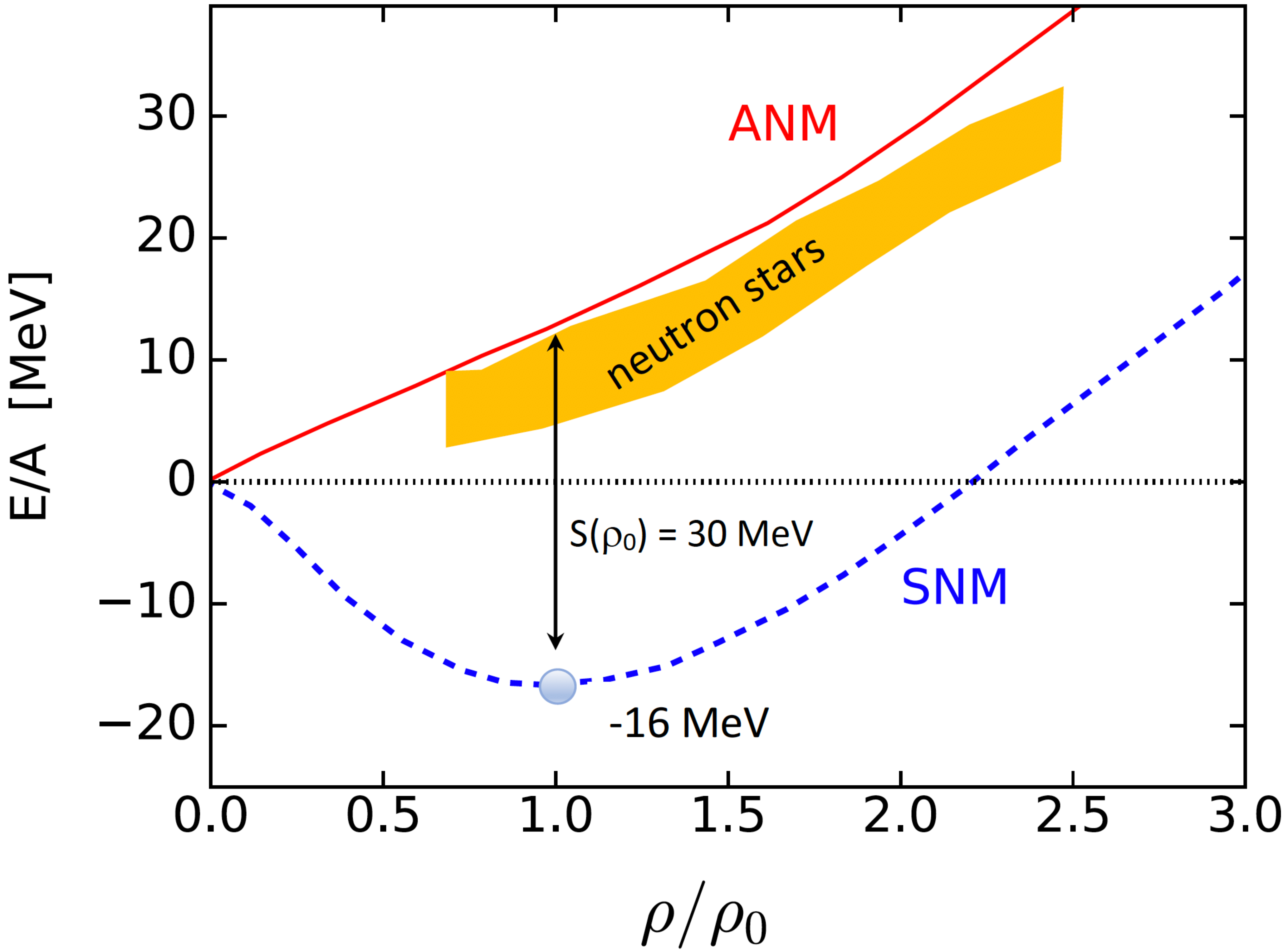

EOS & Neutron stars

Pethick, Ravenhall,
ARNPS 45 (1995) 429

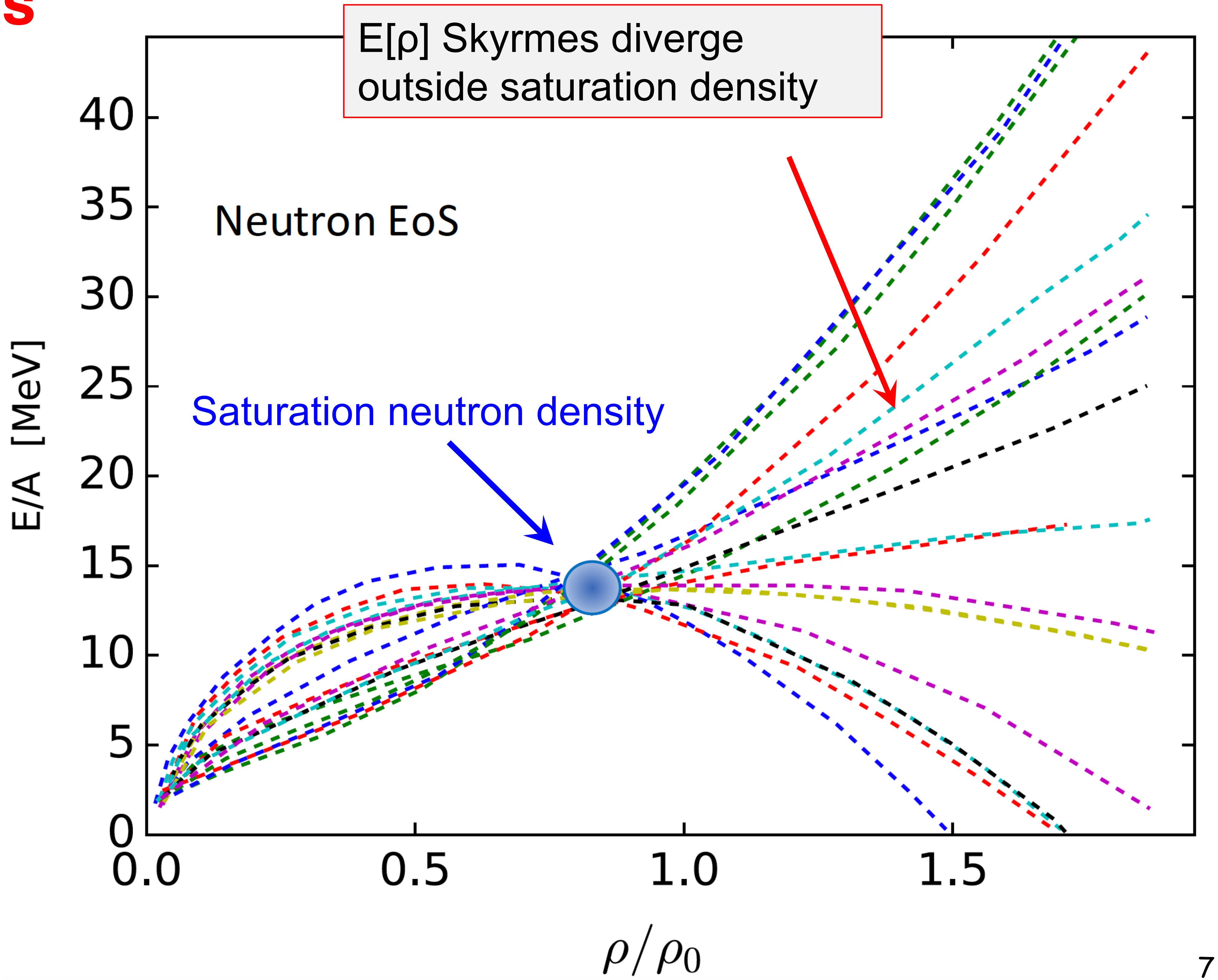

Hyperons and neutron stars

Hyperons make the EoS softer → reduction of the mass

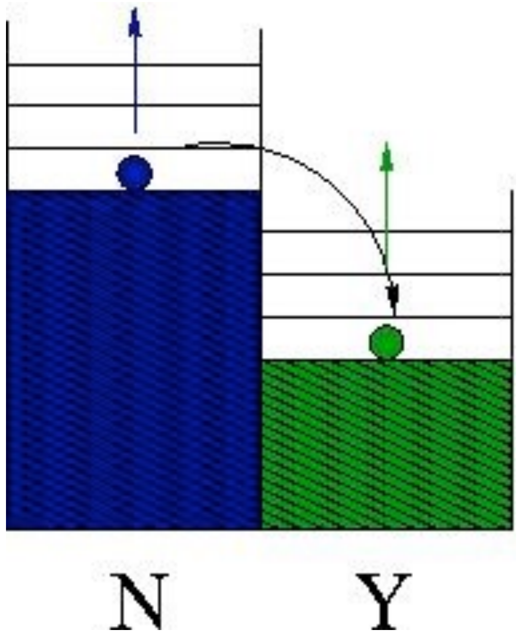

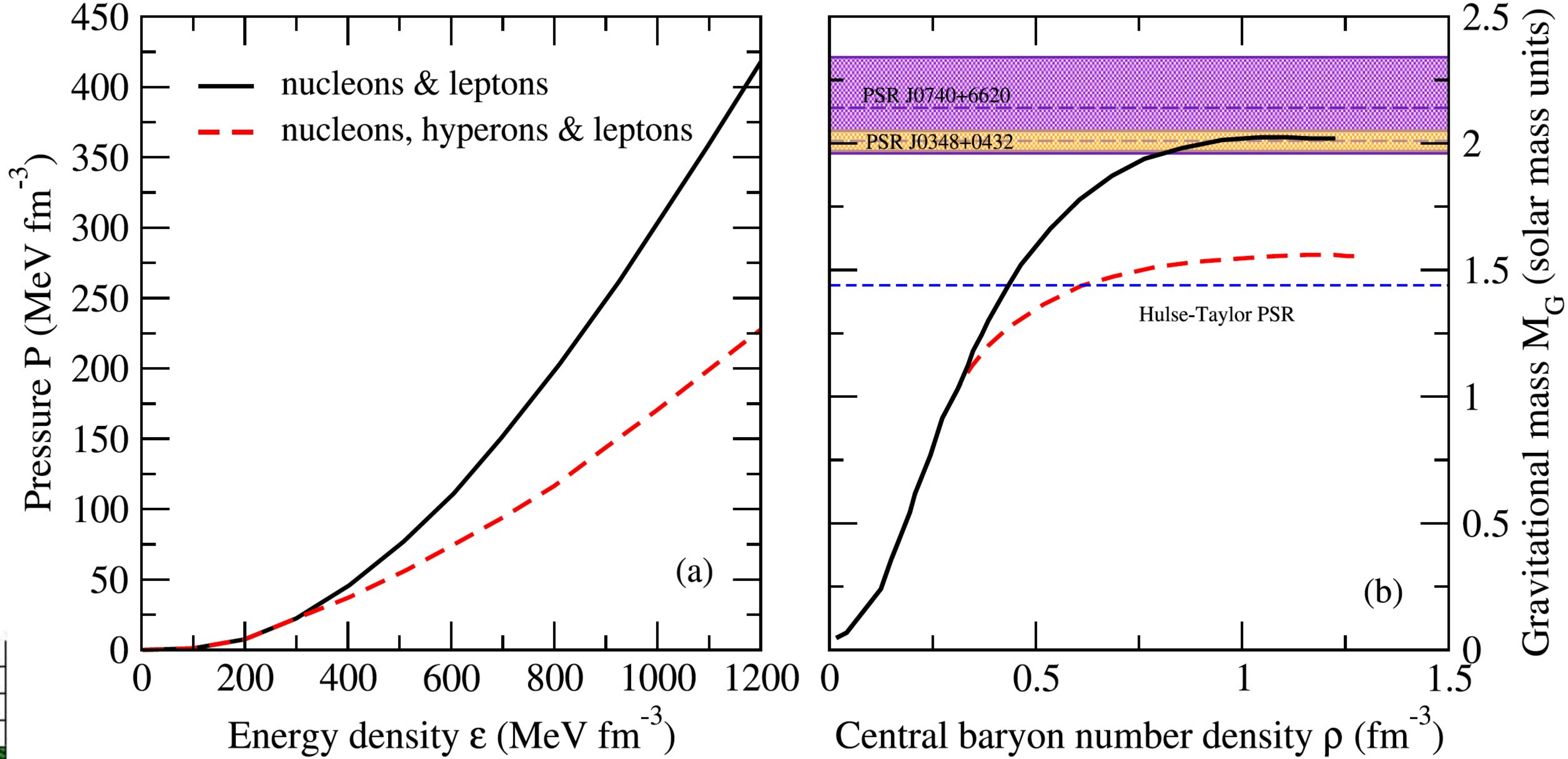

Hyperon "puzzle"

Tolos, Fabbietti, PPNP 112 103770 (2020)

NN interactions and NΛ interactions

Duer, et al.,
Nature 606, 678 (2022)

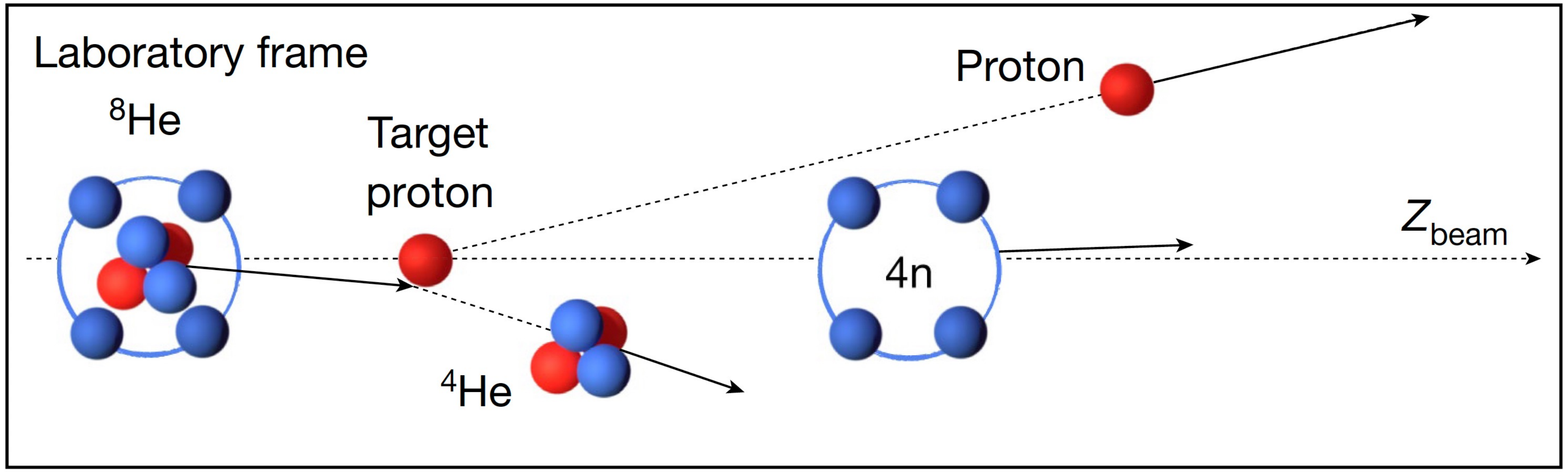

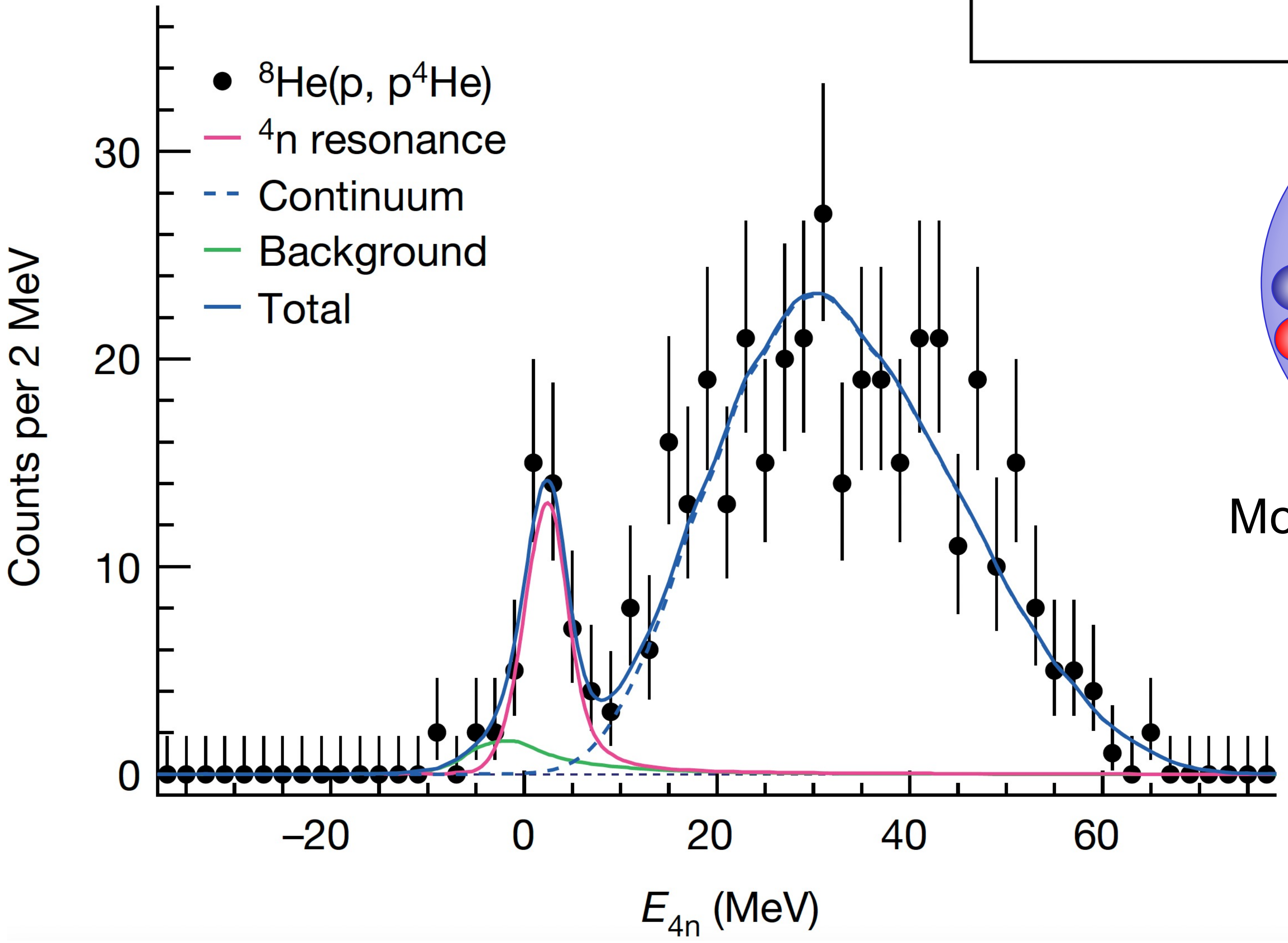

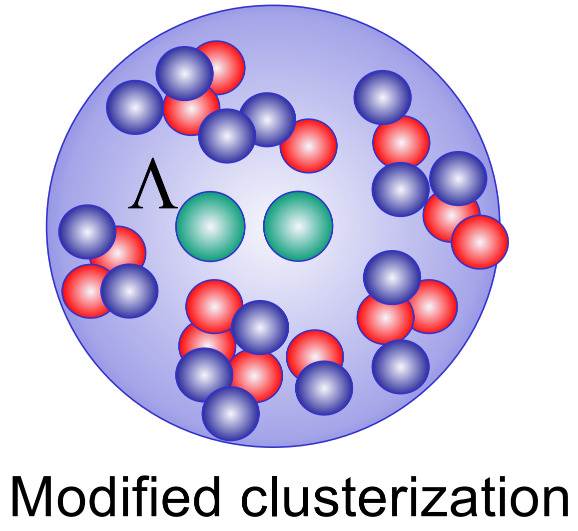

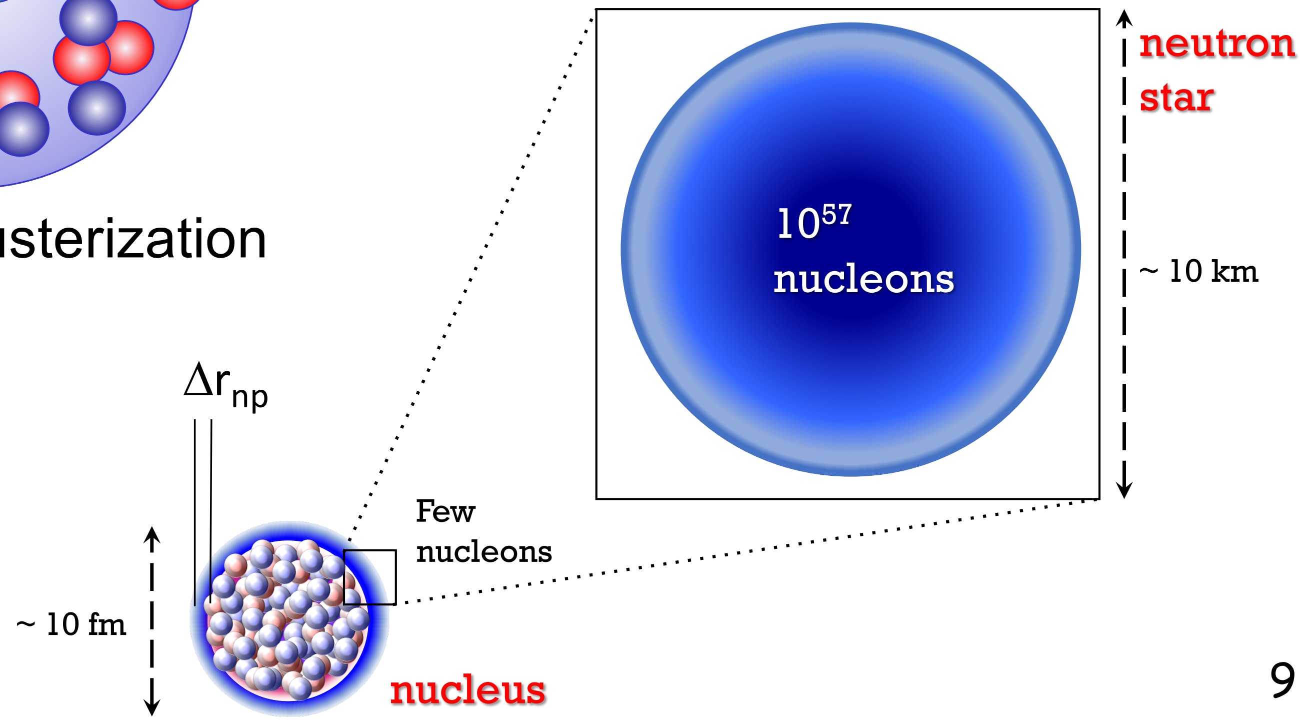

Hypertriton and ΛN interaction

$\tau_\Lambda = 263$ ps
$\tau_{{}^3_\Lambda H} = 253 \pm 11(\text{stat.}) \pm 6(\text{sys.})$ ps

Philipp Eckert, et al., EPJ Web Conf. 271 (2022) 01006

https://hypernuclei.kph.uni-mainz.de

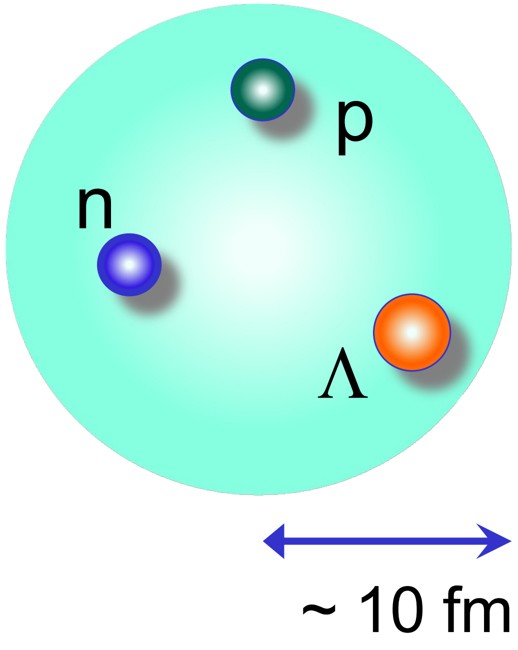

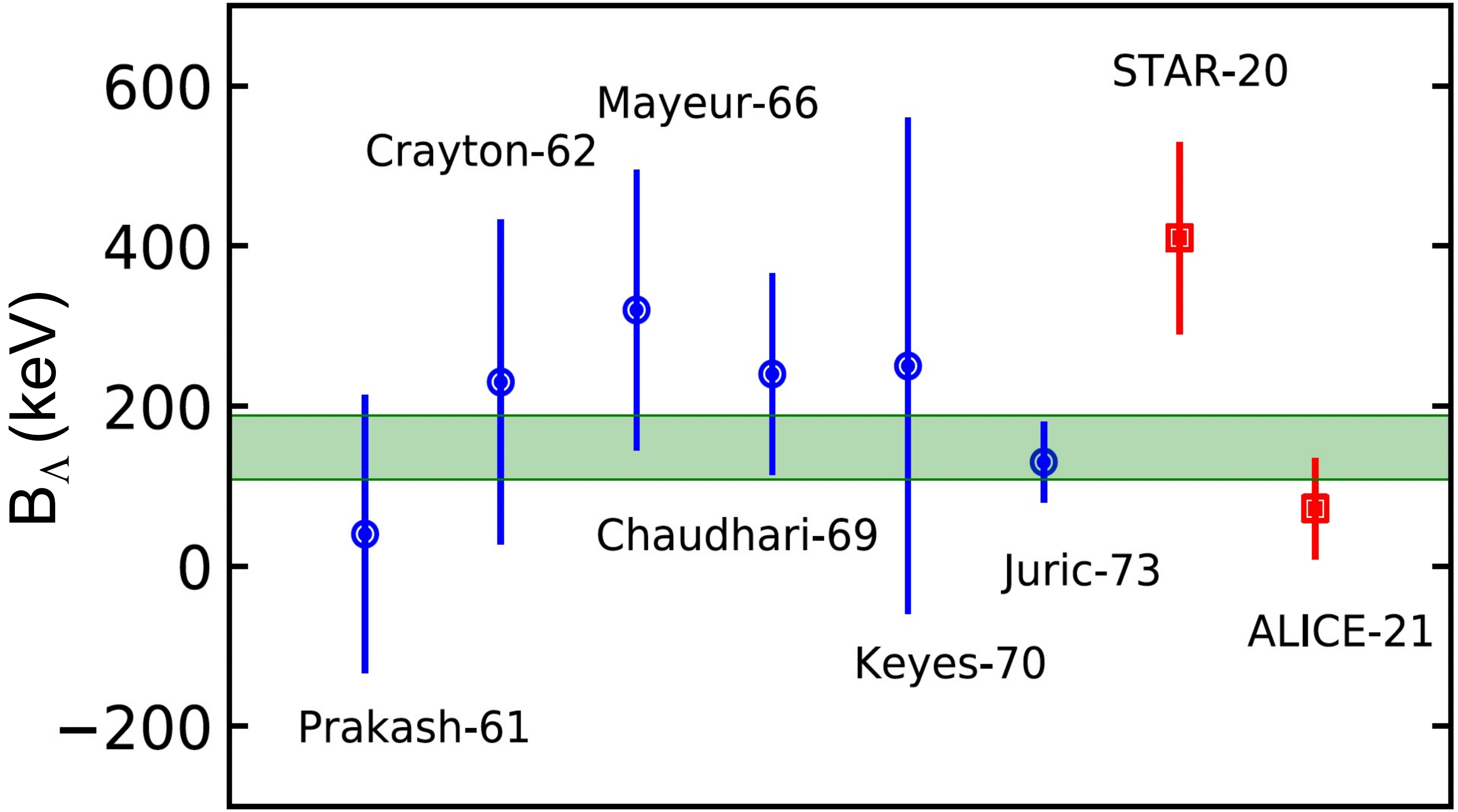

Halo

${}^6_\Lambda$He (S_n = 0.17 MeV)
${}^7_\Lambda$Be(S_{2p} = 0.67 MeV)

Nuclear halos and interaction radius

Tanihata et al.,
PRL 55, 2676 (1985)

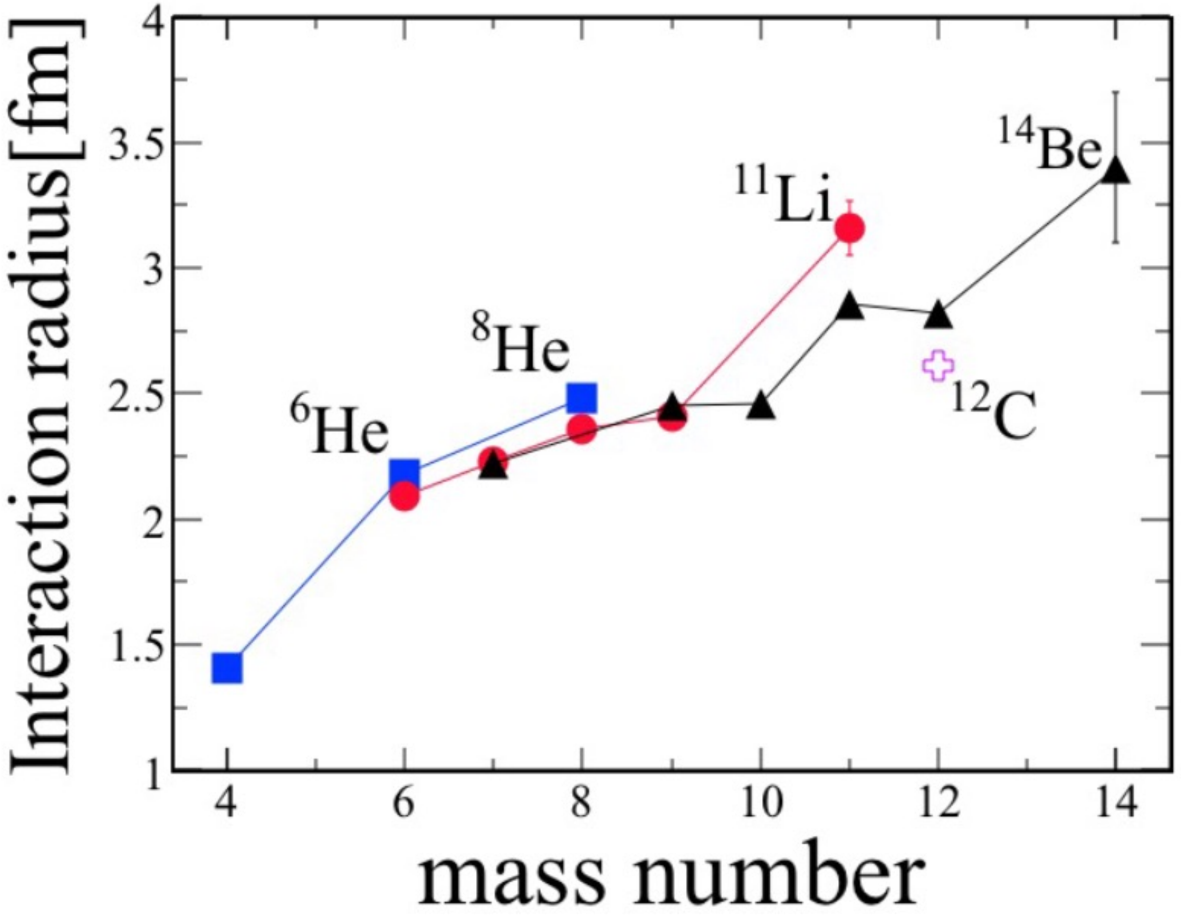

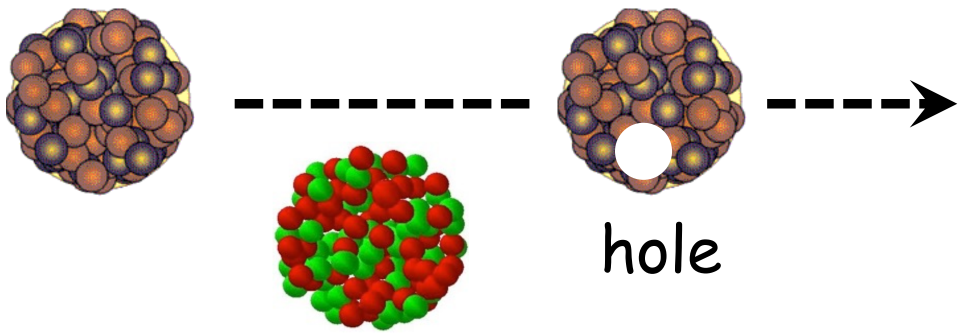

$$\sigma_I = \pi[R_I(P) + R_I(T)]^2$$

^{6}He

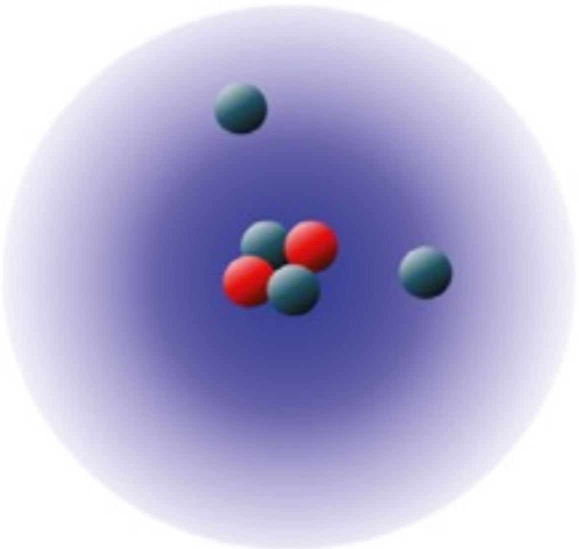

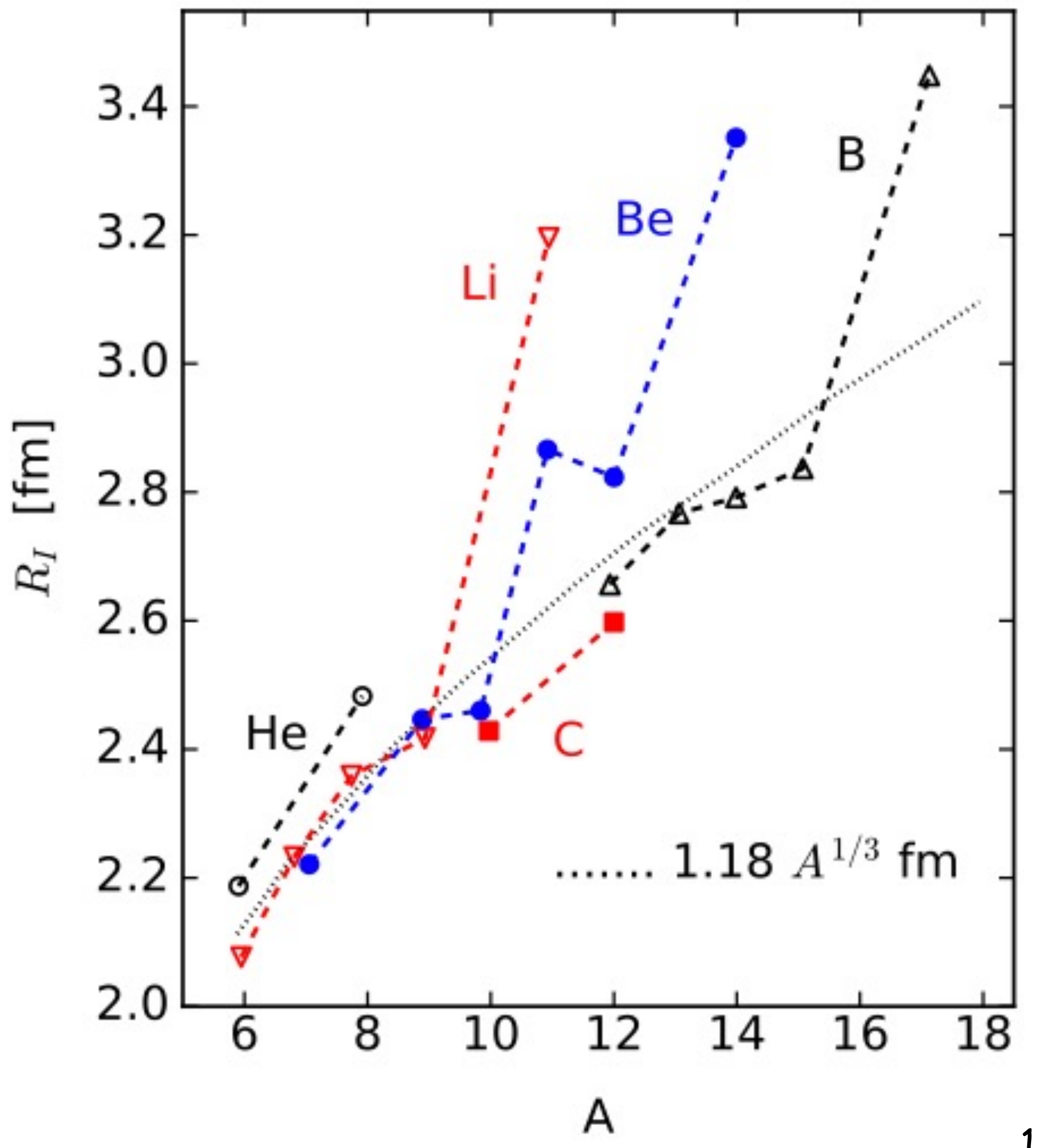

Production of hypernuclei

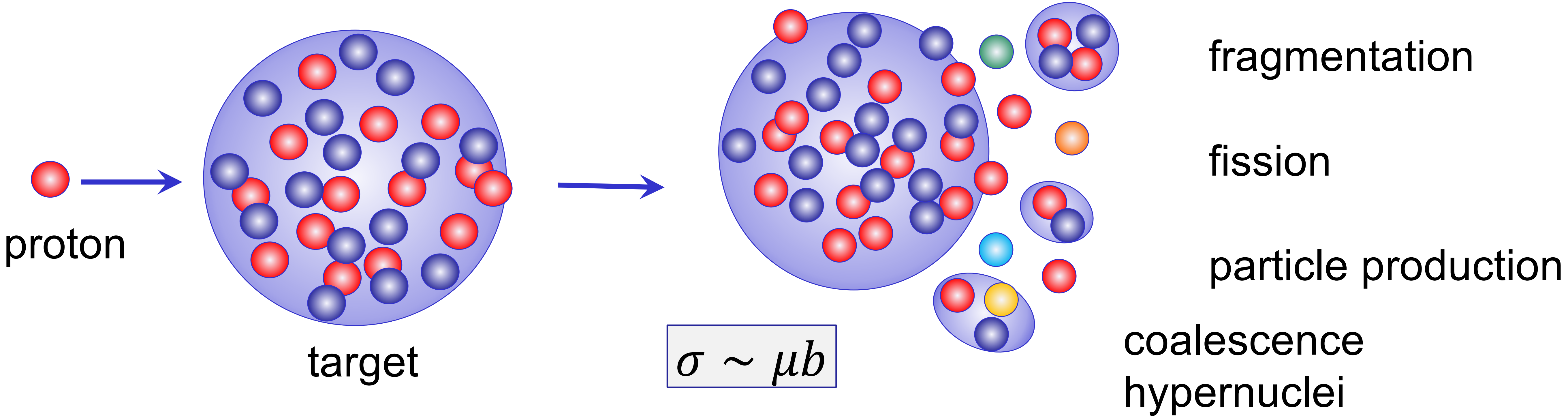

$$C_A = \frac{2J_A + 1}{2^A} \frac{1}{\sqrt{A} m_T^{A-1}} \left(\frac{2\pi}{R^2 + \left(\frac{r_A}{2}\right)^2} \right)^{\frac{3}{2}(A-1)}$$

Particles produced coalesce into nuclei if they are close in space and momentum.

R = source size, r_A = nuclear size
m_T = transverse mass of coalesc. part.

Production & Decay of Hypertriton

Use active target to:
(a) Produce hypertriton
(b) Reconstruct hypertriton by measuring weak decay (${}^{3}_{\Lambda}\mathrm{H} \rightarrow \pi^{-} + {}^{3}\mathrm{He}$)
(c) Interaction cross section though meson decay vertex distribution

Velardita et al.,
Eur. Phys. J. A 59,139 (2023)

$\sigma_I = \sigma_{\Lambda R} \sim 1.8$ b

$\tau \sim 200$ ps

Experiment $\rightarrow \sigma_I \rightarrow R_{{}^{3}_{\Lambda}\mathrm{H}}$

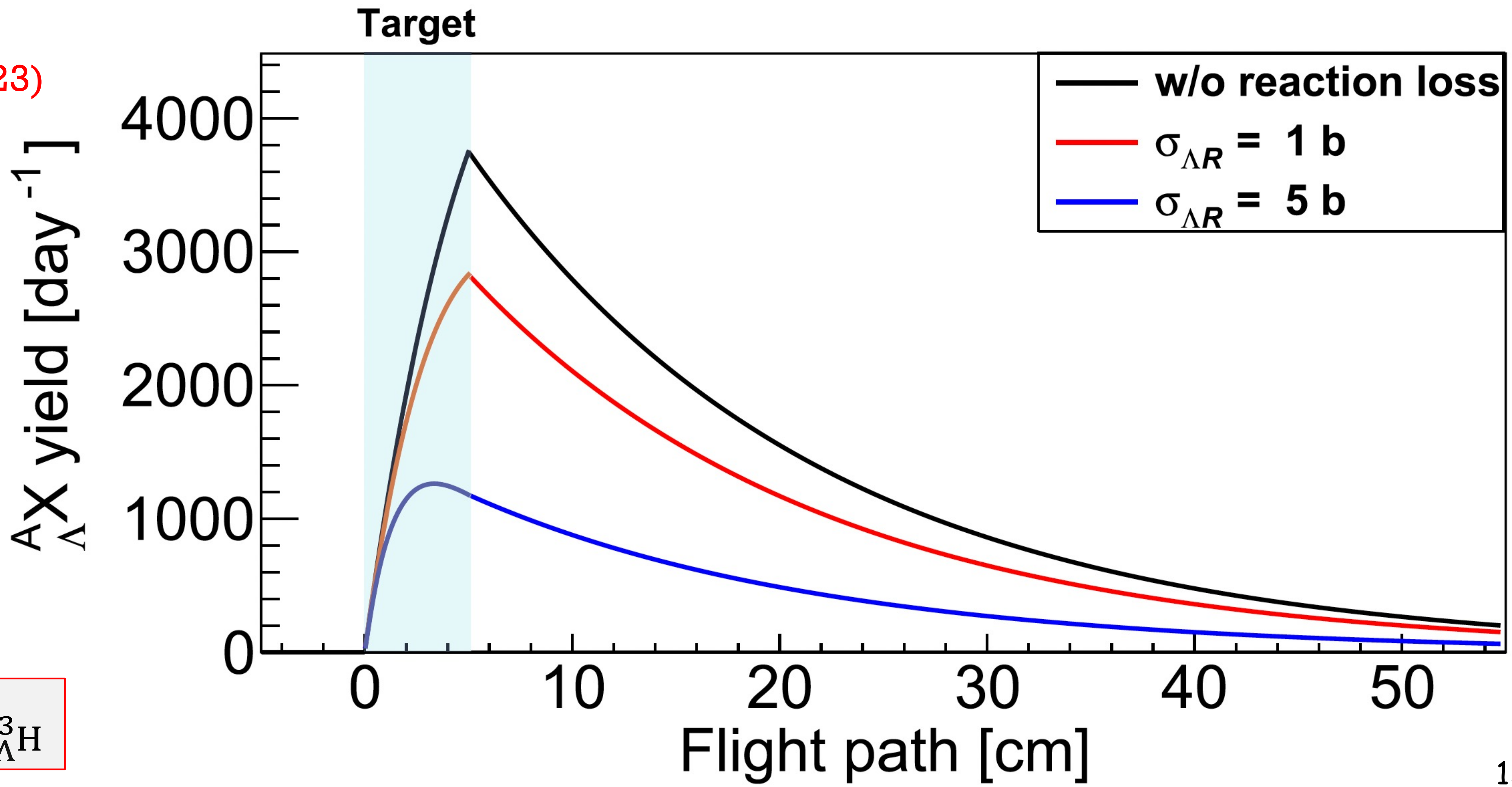

Extraction of Hypertriton radius

Velardita et al.,
Eur. Phys. J. A 59,139 (2023)

$^{12}C + ^{12}C$ collisions
at 1.9 GeV/nucleon

L = active target width

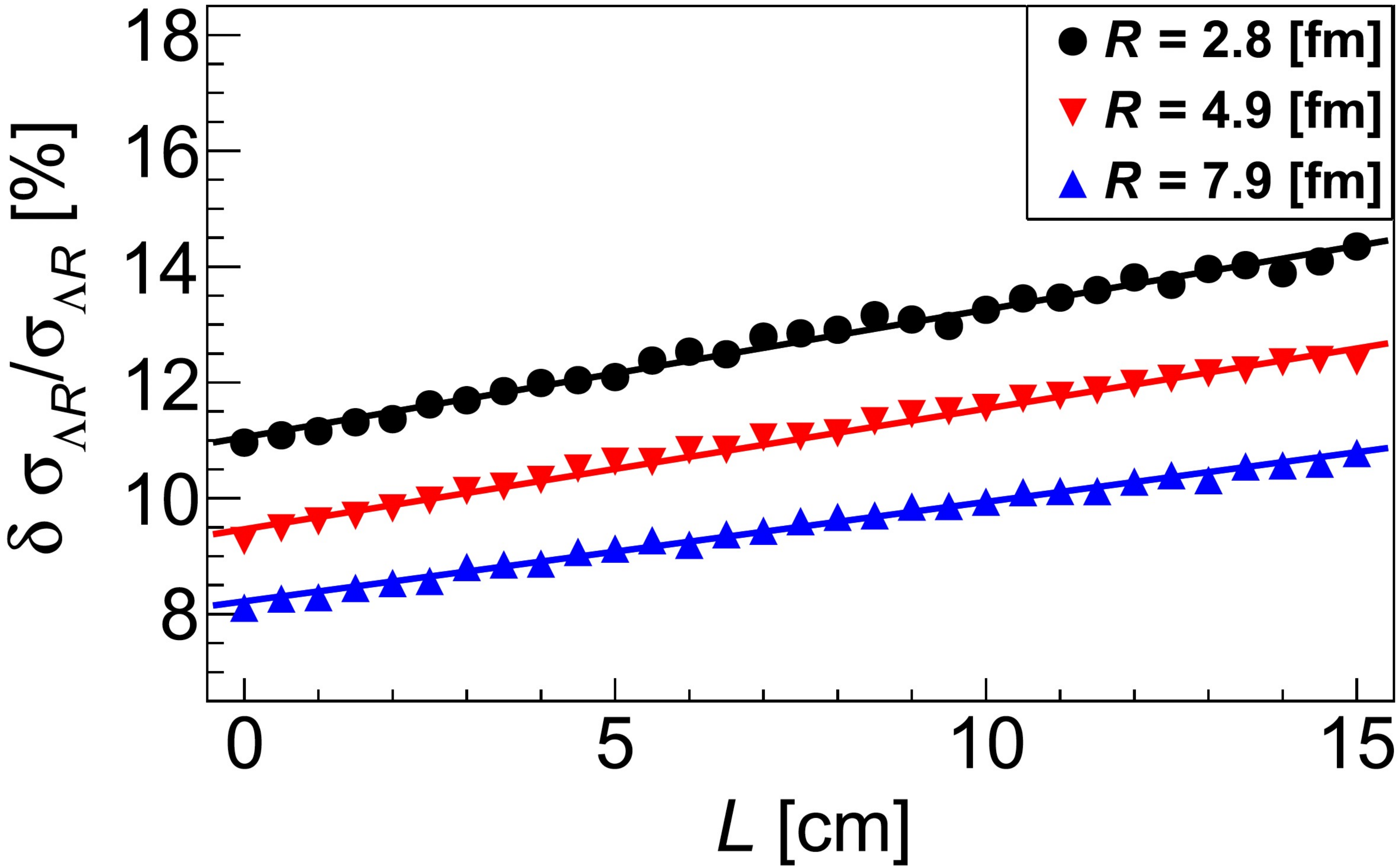

Hypertriton wavefunction

Pionless EFT
(a) Momentum scales < pion mass
(b) Dibaryon field Δ_d
(c) Cutoff parameter Λ_c
(d) Simplified 3-body force $H(s_0,\Lambda_c)$
(e) Asymptotic analysis

$$\begin{aligned}\mathcal{L} =& N^\dagger\left(i\partial_t+\frac{\nabla^2}{2M}\right)N+\Lambda^\dagger\left(i\partial_t+\frac{\nabla^2}{2M_\Lambda}\right)\Lambda \\ &+\Delta_d d_l^\dagger d_l-\frac{g_d}{2}\left[d_l^\dagger N^T\left(i\tau_2\right)\left(i\sigma_l\sigma_2\right)N+\mathrm{H.c.}\right] \\ &+\Delta_s s_j^\dagger s_j-\frac{g_s}{2}\left[s_j^\dagger N^T\left(i\tau_j\tau_2\right)\left(i\sigma_2\right)N+\mathrm{H.c.}\right] \\ &+\Delta_3\left(u_l^3\right)^\dagger u_l^3-g_3\left[i\left(u_l^3\right)^\dagger\Lambda^T\left(i\sigma_l\sigma_2\right)N+\mathrm{H.c.}\right] \\ &+\Delta_1\left(u^1\right)^\dagger u^1-g_1\left[i\left(u^1\right)^\dagger\Lambda^T\left(i\sigma_2\right)N+\mathrm{H.c.}\right]+\ldots\end{aligned}$$

Hildenbrand, Hammer,
Phys. Rev. C, 100, 034002 (2019)

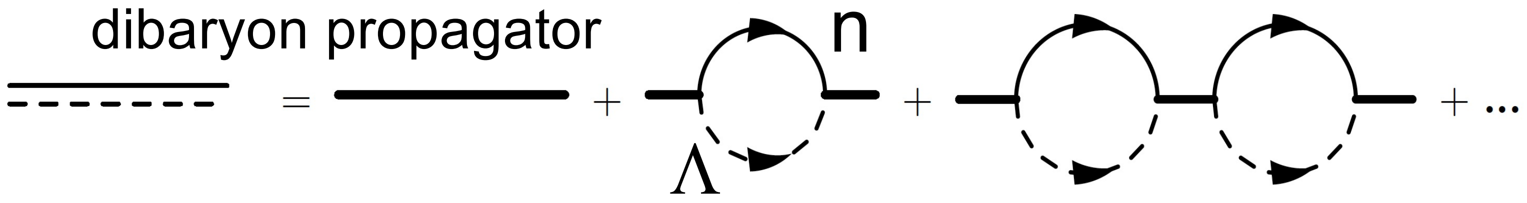

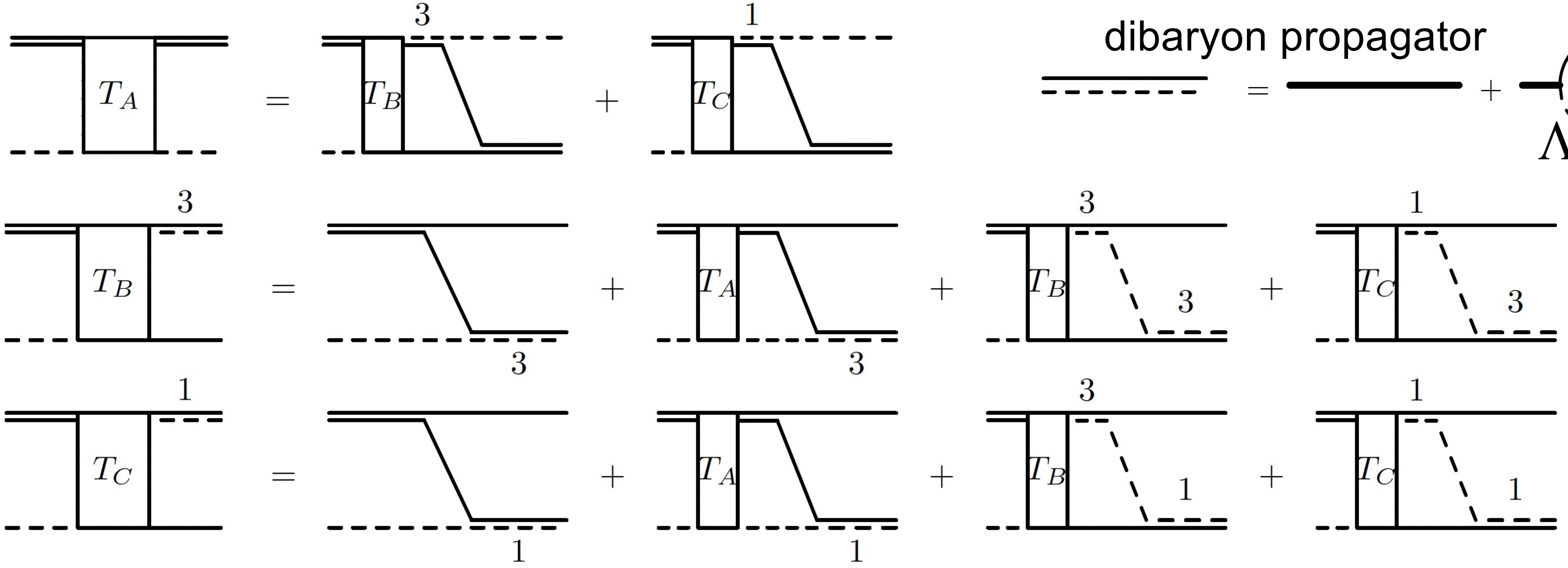

Hypertriton wavefunction (EFT)

$\sqrt{\langle r^2_{\Lambda-NN'}\rangle}$[fm]	$\sqrt{\langle r^2_{N'-\Lambda N}\rangle}$[fm]	$\sqrt{\langle r^2_{NN'}\rangle}$[fm]
10.79	3.96	2.96
$+3.04/-1.53$ $+0.03/-0.02$	$+0.40/-0.25$ $+0.03/-0.03$	$+0.06/-0.05$ $+0.03/-0.04$

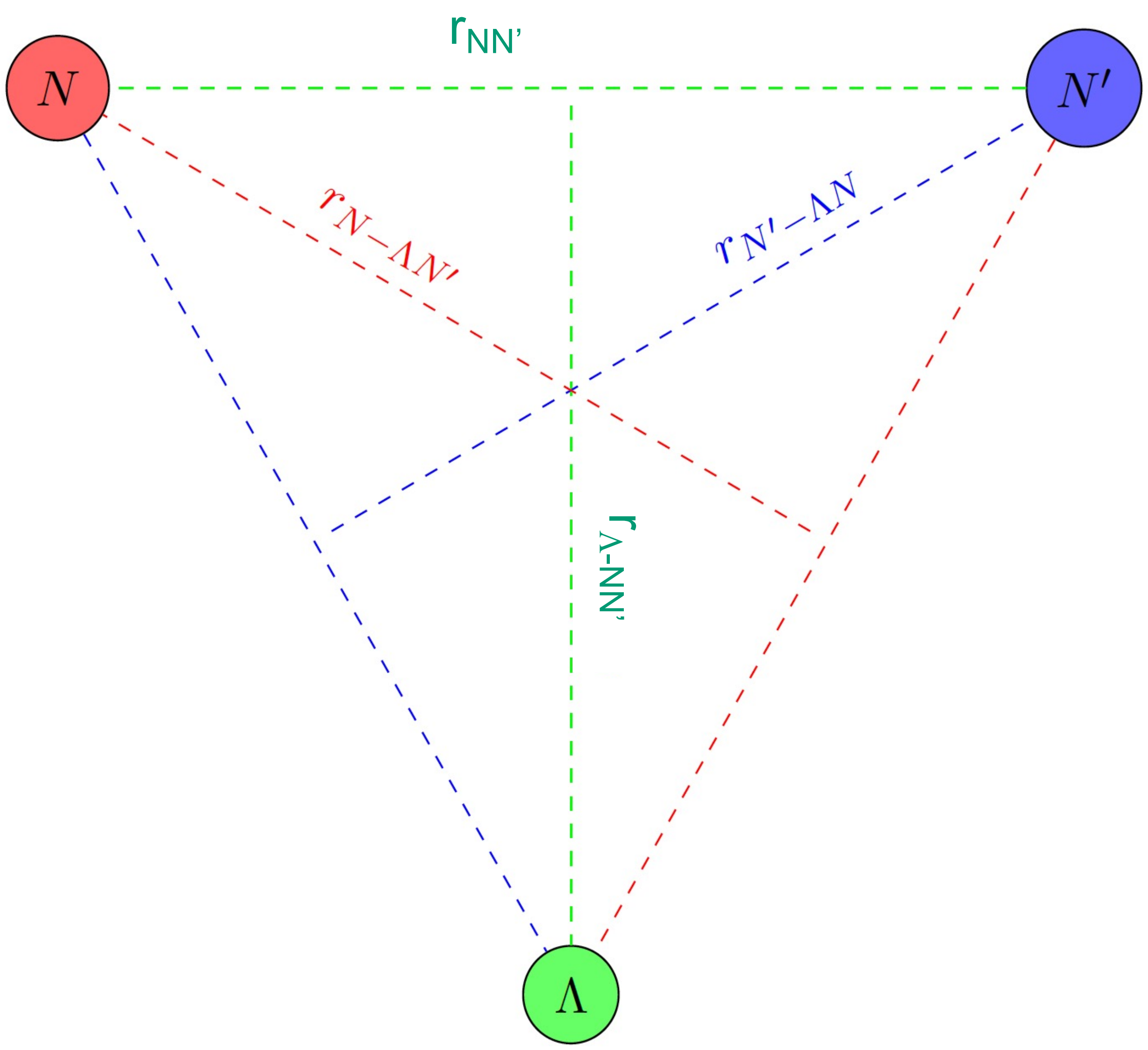

Confirms that the "picture" as a **two body system** consisting of a deuteron and a Λ is a good approximation.

Congleton, JPG 18, 339 (1992)
+ many others

Hypertriton wavefunction

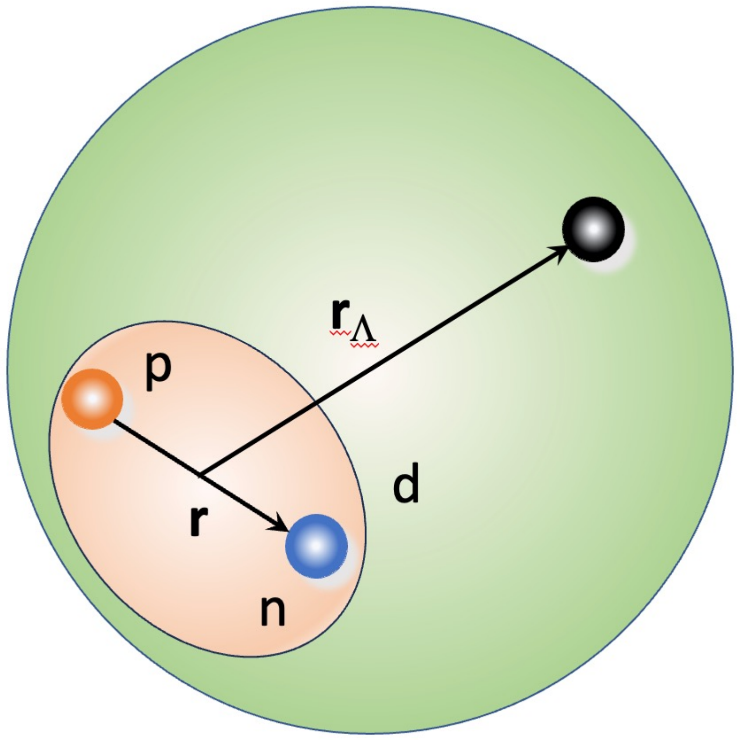

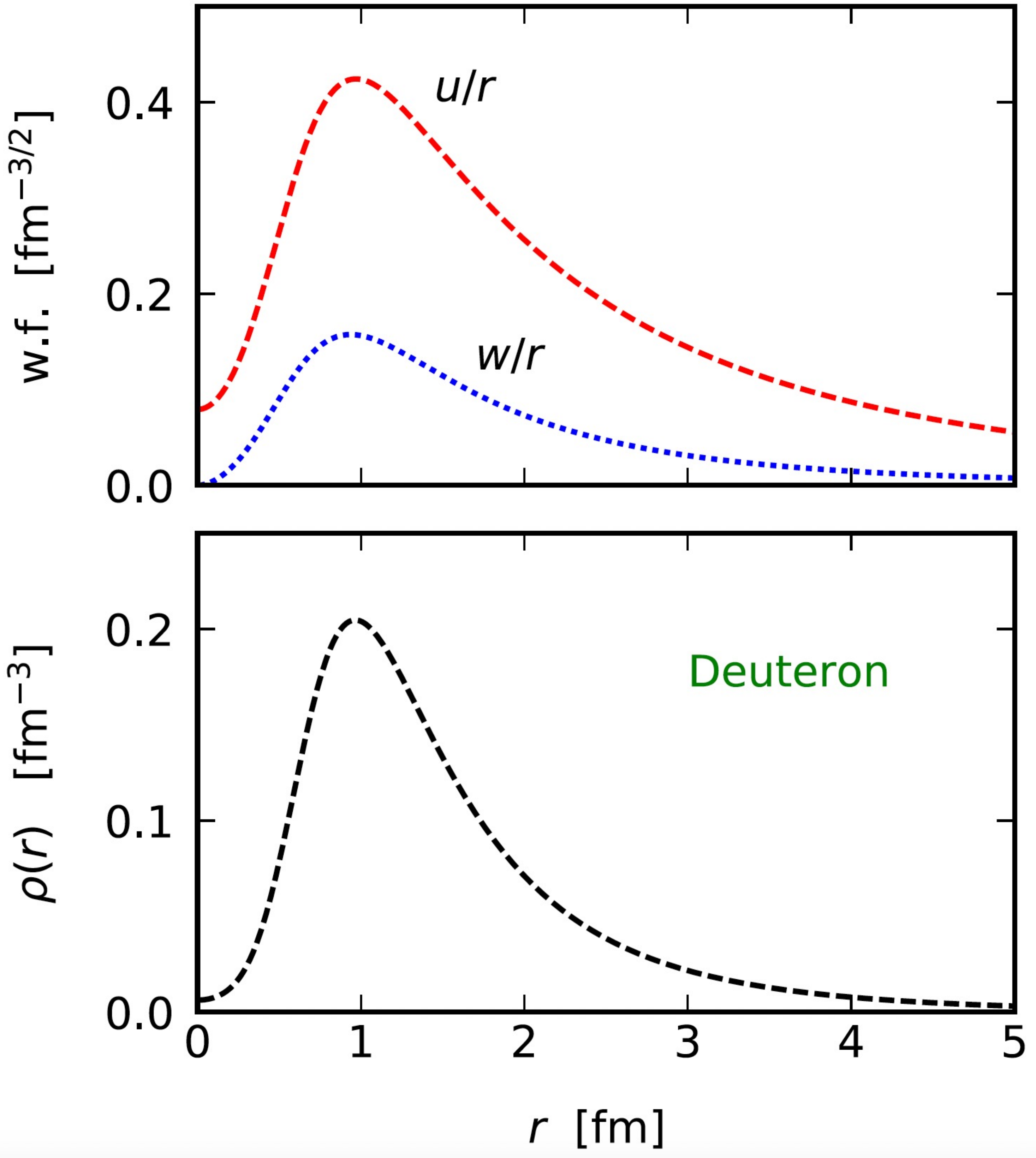

Deuteron radial s-wave, $u(r)/r$, and d-wave, $w(r)/r$ as a function of the proton-neutron distance r using Av18 interaction.

Wiringa, Stoks, Schiavilla
Phys. Rev. C 51, 38 (1995)

Hypertriton wavefuncti

CB, PLB 837, 137639 (2023)

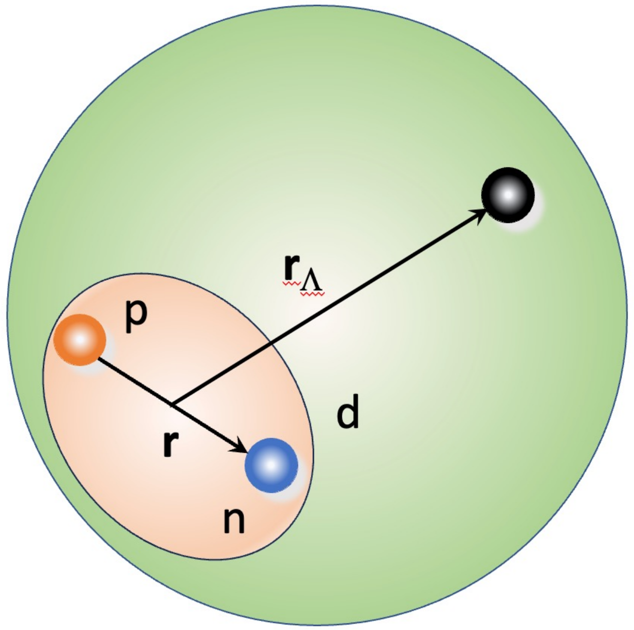

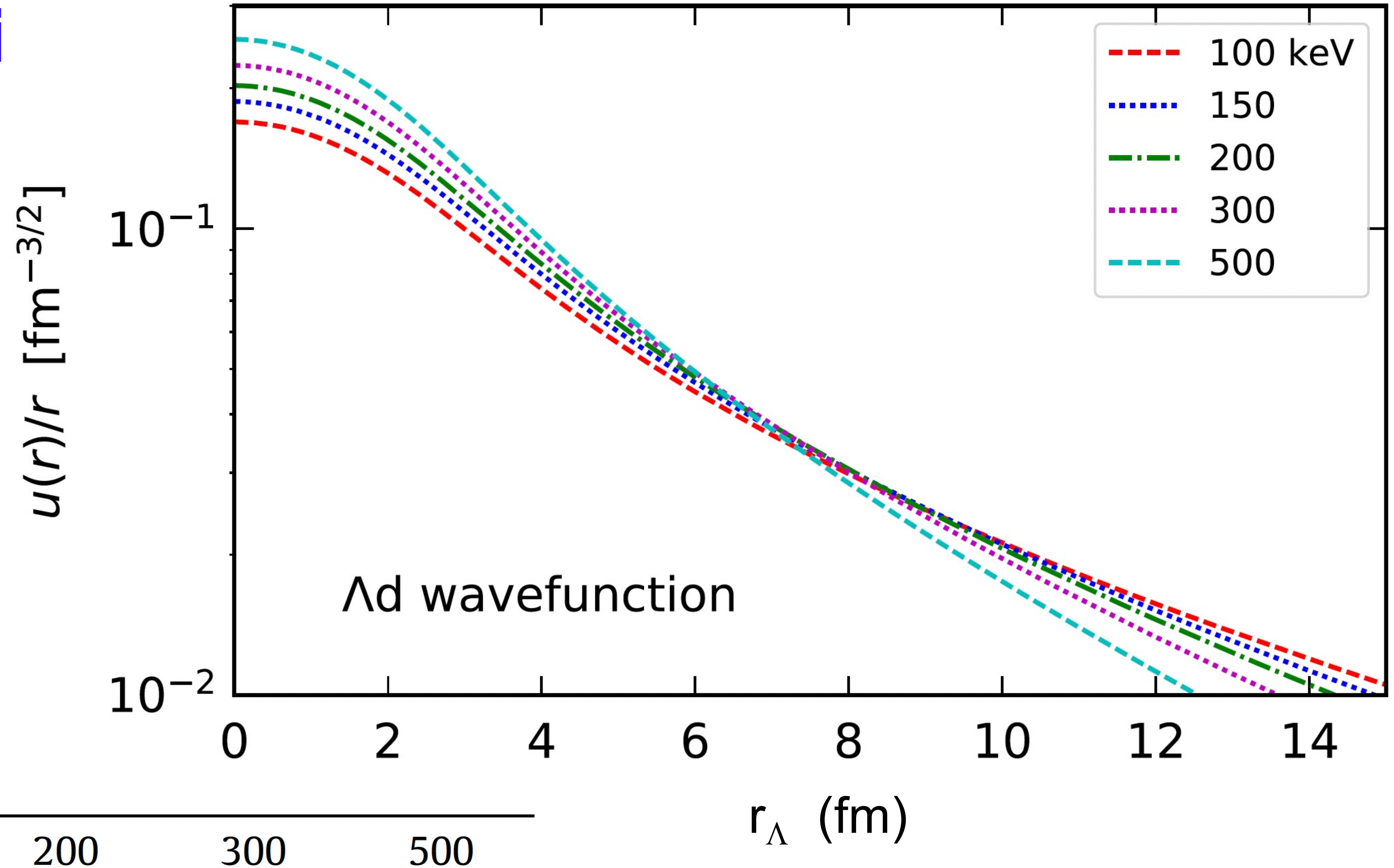

B_Λ (keV)	100	150	200	300	500
V_0 [MeV]	-11.8	12.2	-12.6	-13.2	-14.3

Λ-deuteron wavefunction - Woods-Saxon, radius R = 2.5fm, diffuseness a = 0.65 fm.

u(r)/r for the s-wave and binding energies B = 100, 150, 200, 300 and 500 keV.

Hypertriton + nucleon density

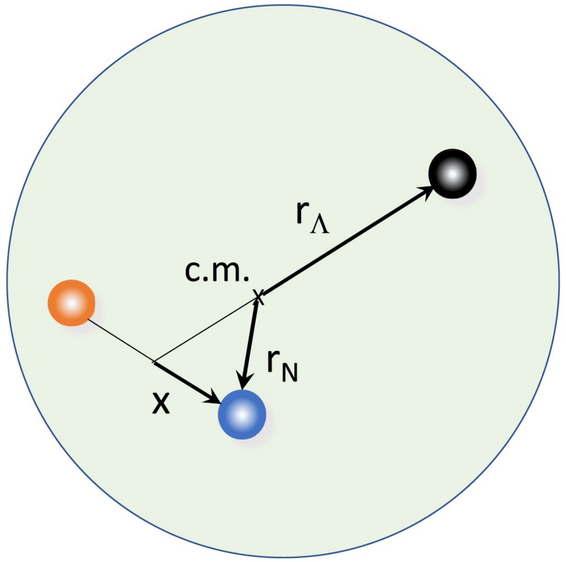

$$\alpha = \frac{m_d}{m_\Lambda + m_d}$$

$$\beta = \frac{m_\Lambda}{m_\Lambda + m_d}$$

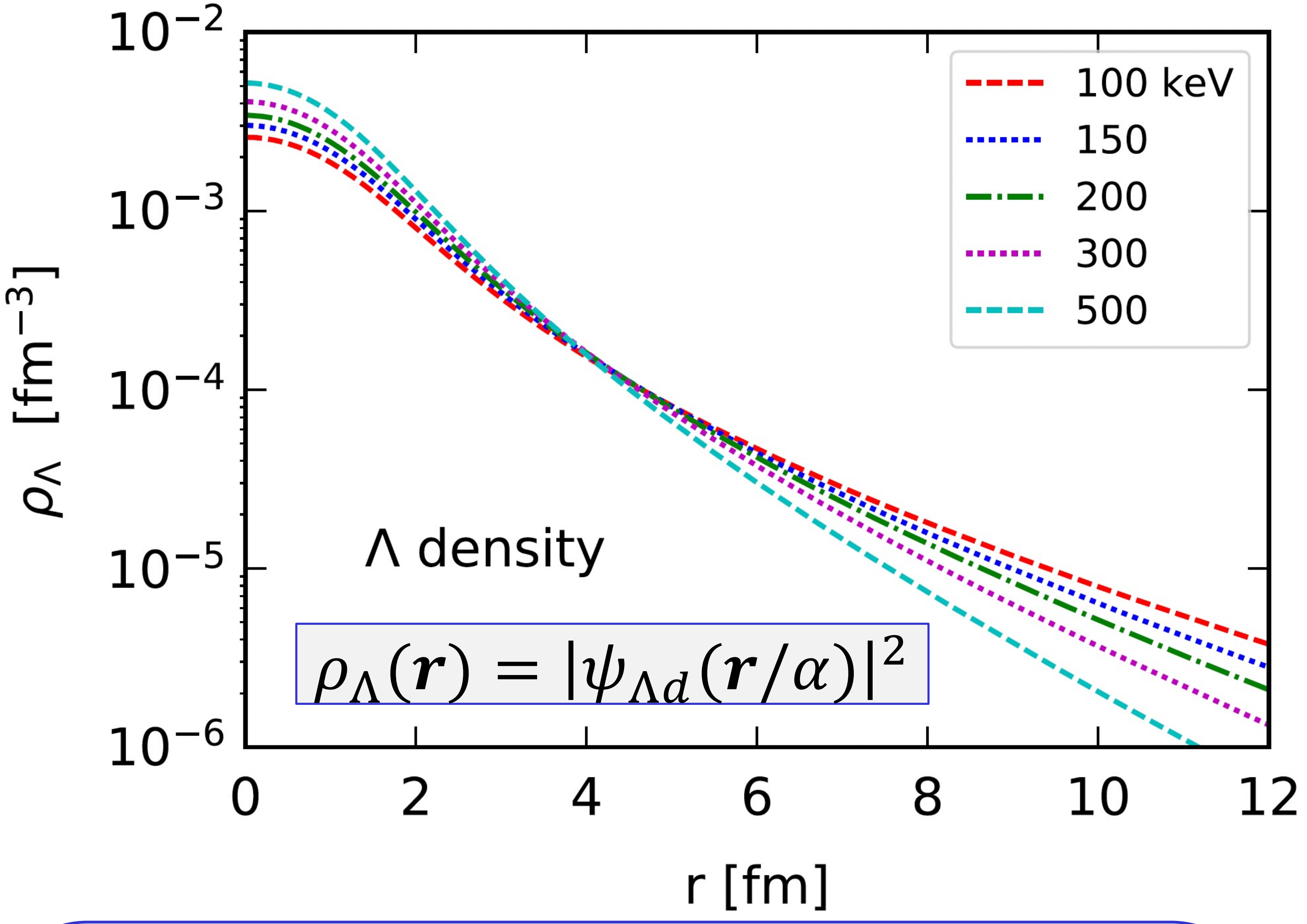

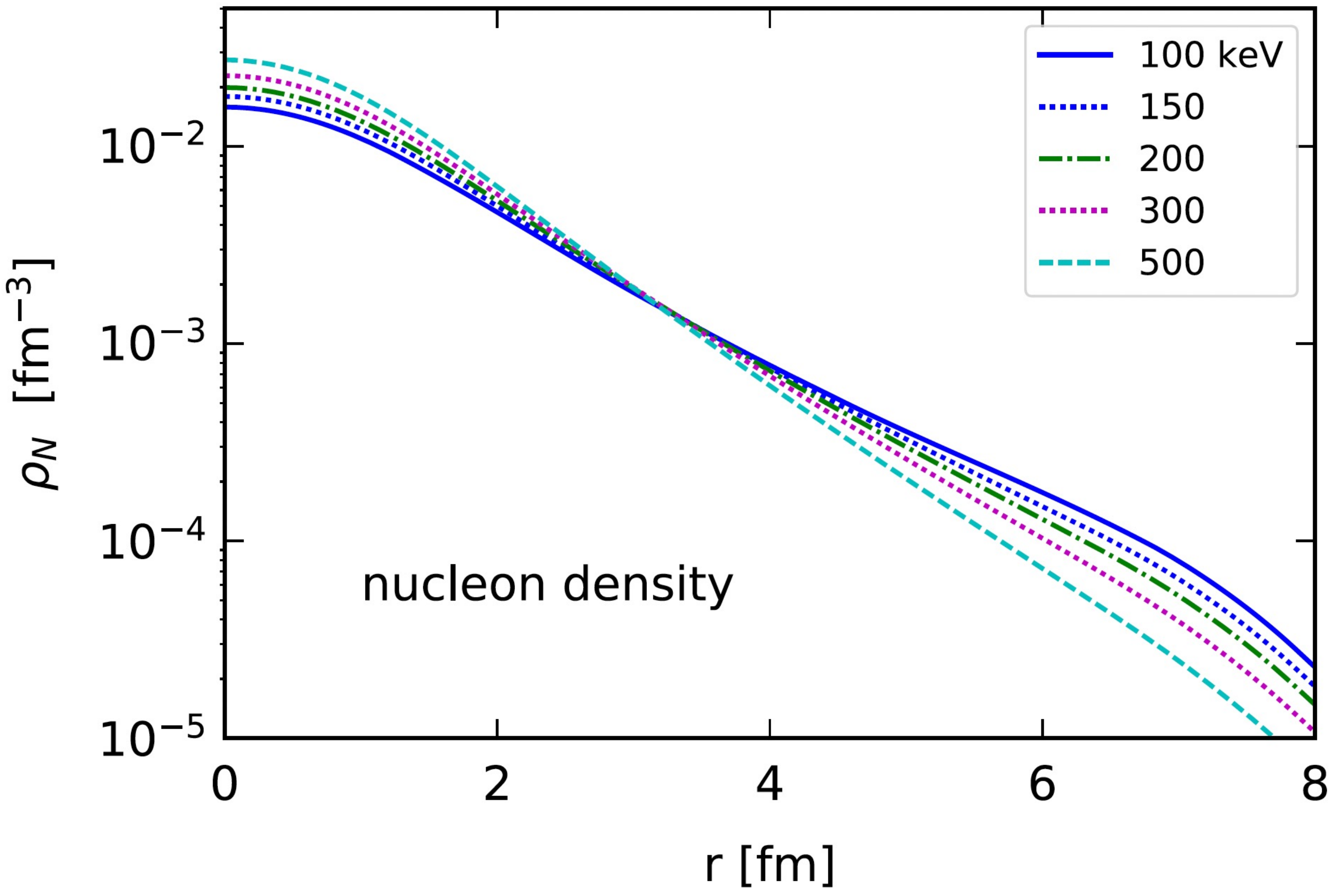

$\rho_1(\boldsymbol{r}_\Lambda) = |\psi_{\Lambda d}(\boldsymbol{r}/\beta)|^2$ Λ dist. within ${}^3_\Lambda\mathrm{H}$

$\rho_2(\boldsymbol{r}_p) = \left|\psi_{deut}^{free}(2\boldsymbol{x})\right|^2$ p dist. within deut.

$\rho_N(\boldsymbol{r}_N) = \int \rho_1(|\boldsymbol{r} - \boldsymbol{x}|)\, \rho_2(\boldsymbol{x})$

nucleon distribution within ${}^3_\Lambda\mathrm{H}$

Hypertriton destruction

$$T(b) = T_\Lambda(b)\, T_p(b)\, T_n(b)$$

Transmission probability

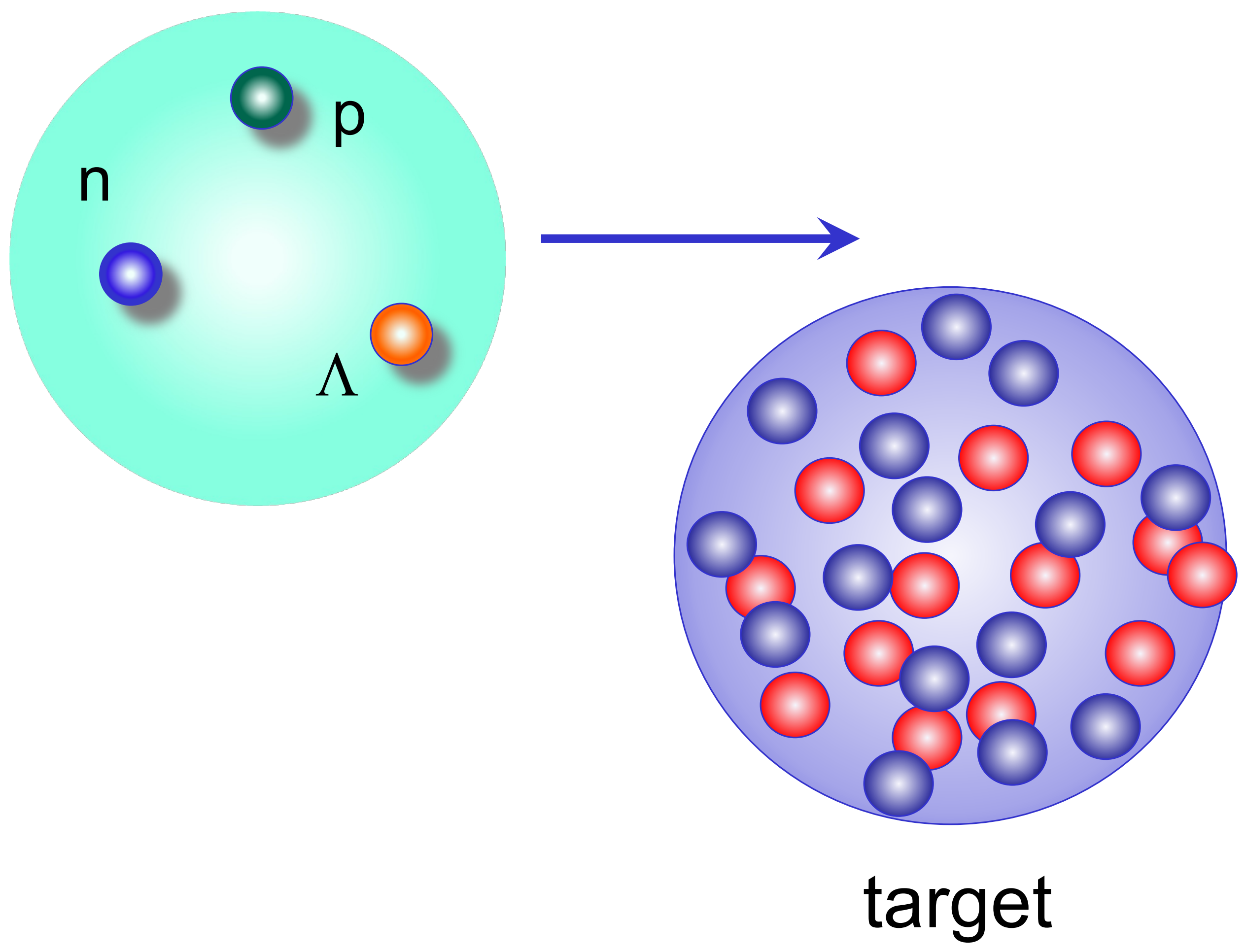

$$T_i(b) = \int d^2 s_i dz_i (z_i, \boldsymbol{s}_i - \boldsymbol{b})$$
$$= \exp\left[-\sigma_{pi} Z_T \int dz'\, \rho_p^T(z', \boldsymbol{s})\right]$$
$$= \exp\left[-\sigma_{ni} N_T \int dz'\, \rho_n^T(z', \boldsymbol{s})\right]$$

$i = \Lambda, p,$ or n

1.5 GeV/nucleon ${}^3_\Lambda$H incident on ^{12}C, ^{120}Sn, ^{208}Pb
$\sigma_{np} = 45.8$ mb
$\sigma_{pp} = 40$ mb
$\sigma_{\Lambda p} = 35$ mb

Hypertriton destruction

Transmission probability

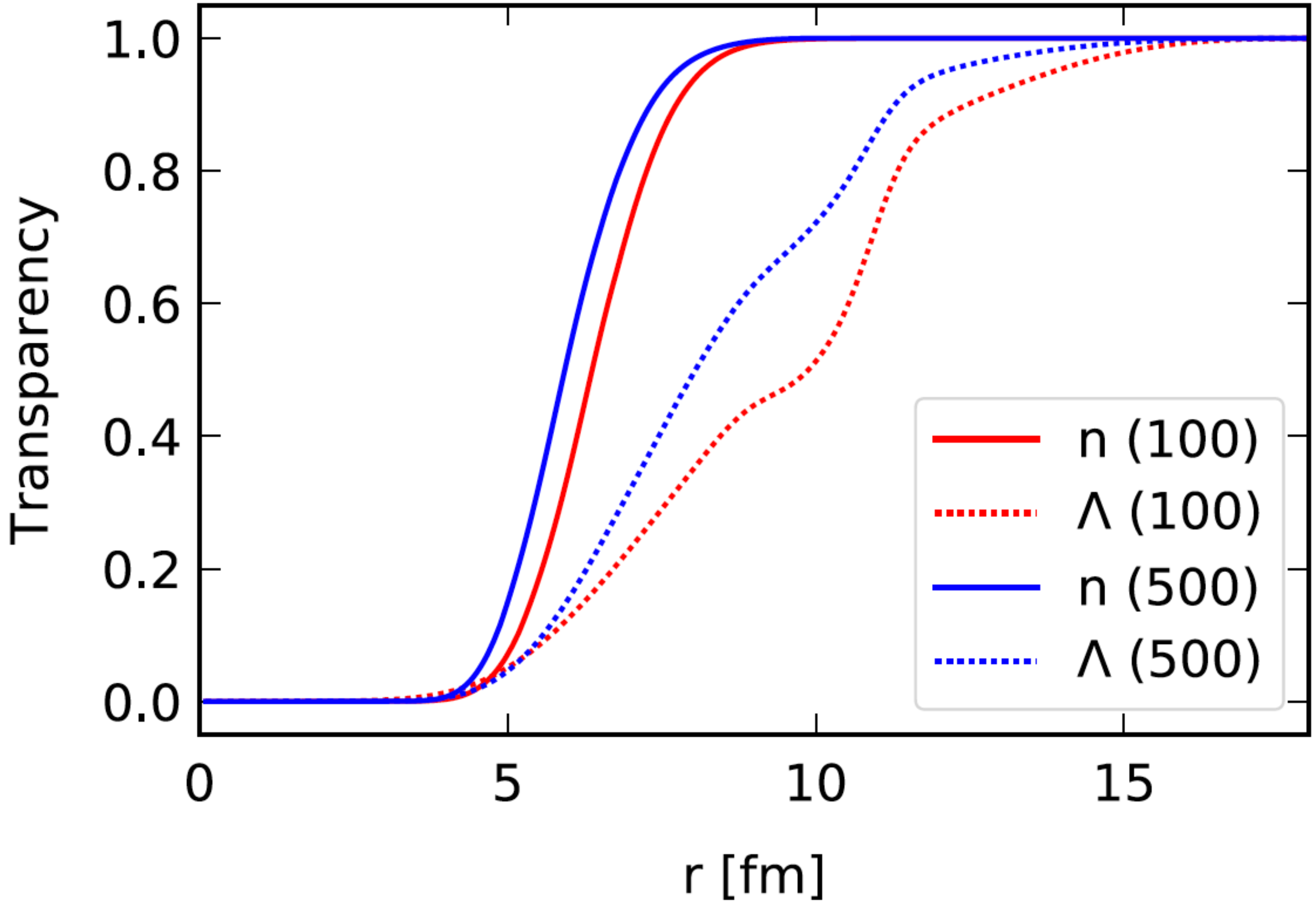

Transition from full opaque-ness to full transparency displays changes in the slope due to structure of the deuteron within ${}^{3}_{\Lambda}$H.

Sensitivity to hypertriton interaction cross sections

1.5 GeV/nucleon ${}^{3}_{\Lambda}$H incident on ^{12}C, ^{120}Sn, ^{208}Pb

B_Λ (keV)	σ_I(C)	σ_I(Sn)	σ_I(Pb)
100	842.	2516.	3098.
150	824.	2424.	2982.
200	807.	2341.	2876.
300	783.	2220.	2721.
500	749.	2043.	2490.

$B_\Lambda = 148 \pm 40$ keV

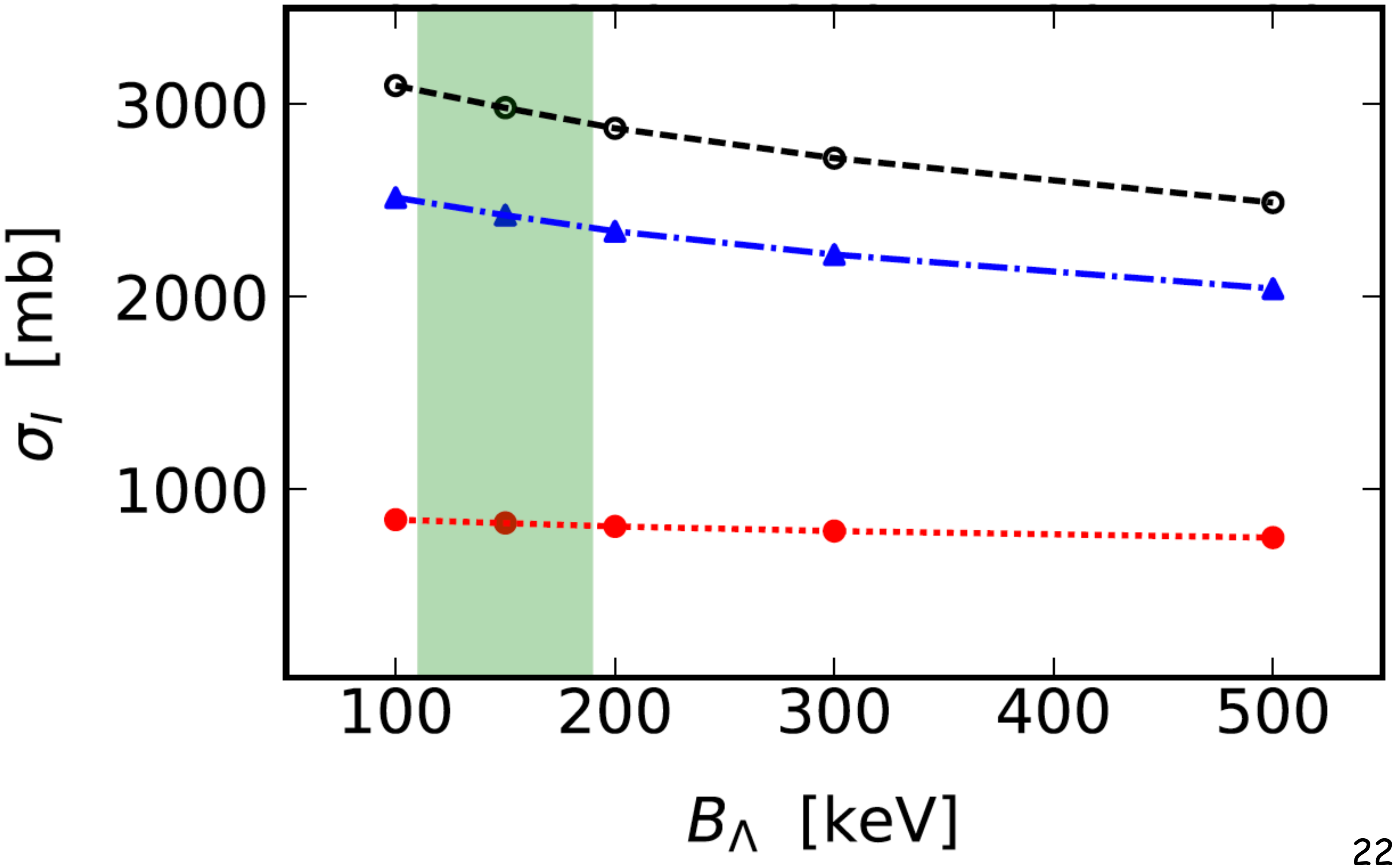

For a C target: a 12% reduction of the cross section $\sigma_{\Lambda I}$ from B = 100 MeV to B = 500 MeV.

Electromagnetic response of the hypertriton

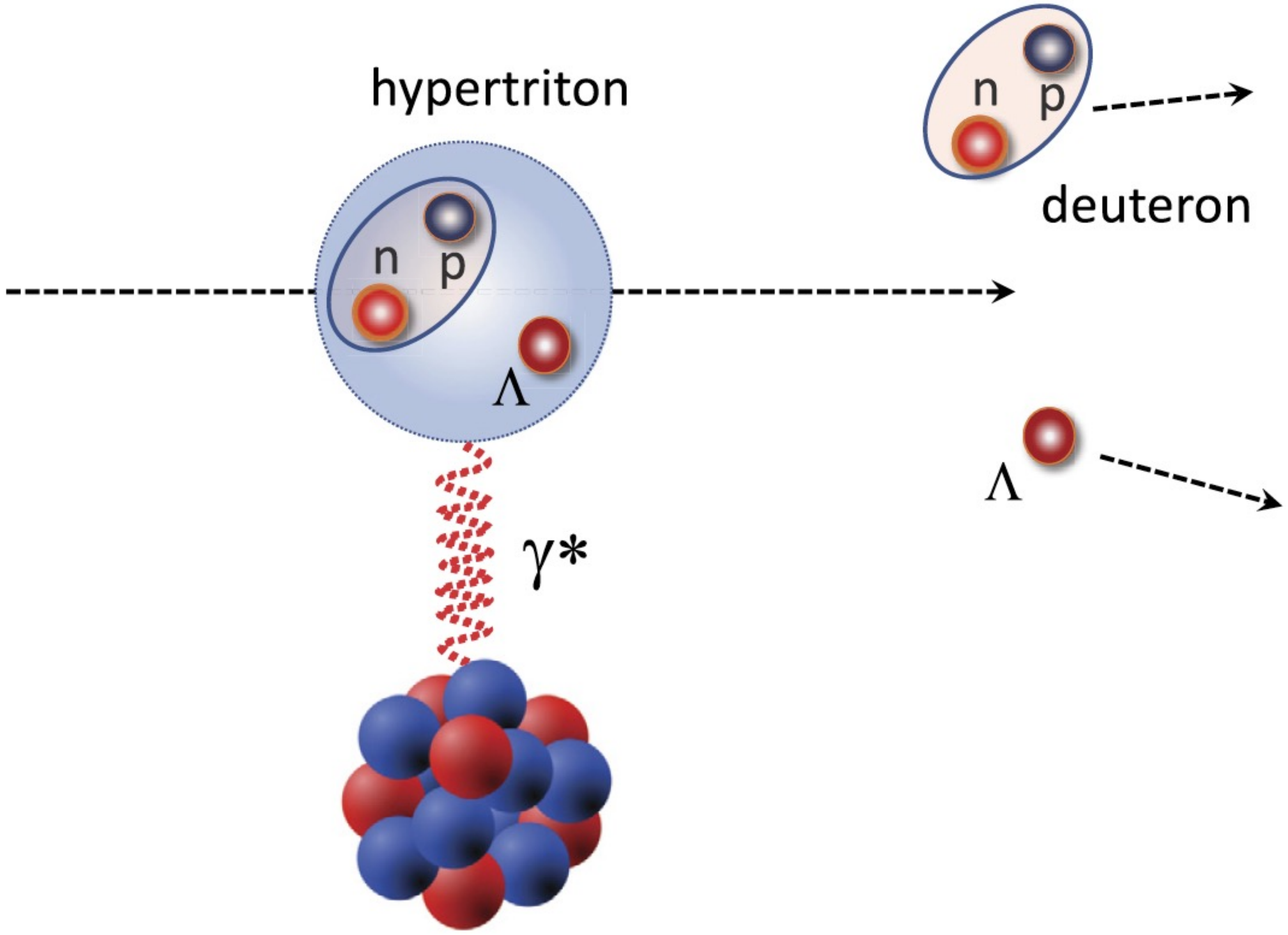

$$\frac{d\sigma_C}{dE} = \frac{16\pi^3}{9\hbar c} n(E) \frac{dB(E)}{dE}$$

$$n(E) = \frac{2Z_T^2\alpha}{\pi}\left(\frac{Ec}{\gamma\hbar v^2}\right)^2 \int_0^\infty dbb\left[K_1^2 + \frac{1}{\gamma^2}K_0^2\right]T(b)$$

$$x = Eb/\gamma v$$

First-order perturbation theory

$$\frac{dB(E)}{dE} = \frac{1}{\hbar}\sqrt{\frac{\mu}{2E}}|\langle g.s.||\mathcal{O}_{E1}||E,l\rangle|^2$$

$$\langle g.s.||\mathcal{O}_{E1}||E,l\rangle = (-1)^l \frac{e_{eff}}{\sqrt{4\pi}}\int_0^\infty dr\, r u_{g.s.}(r) u_{E,l}(r)$$

$$u_{E,l}(r) \rightarrow \sqrt{2\mu_{\Lambda d}/\pi\hbar^2 k}\, e^{i\delta_l}\sin(kr + \delta_l)$$

Electromagnetic response of the hypertriton

$$\frac{dB(E)}{dE} = \frac{1}{\hbar}\sqrt{\frac{\mu}{2E}}\,|\langle g.s.||\mathcal{O}_{E1}||E,l\rangle|^2$$

Analytical model:

CB, Sustich
Phys. Rev. C 46 (1992) 2340

$$\frac{dB(E)}{dE} = C\sqrt{B_\Lambda}\,\frac{E^{3/2}}{(E+B_\Lambda)^4}$$

$$E_{max} = \frac{3}{5}B_\Lambda$$

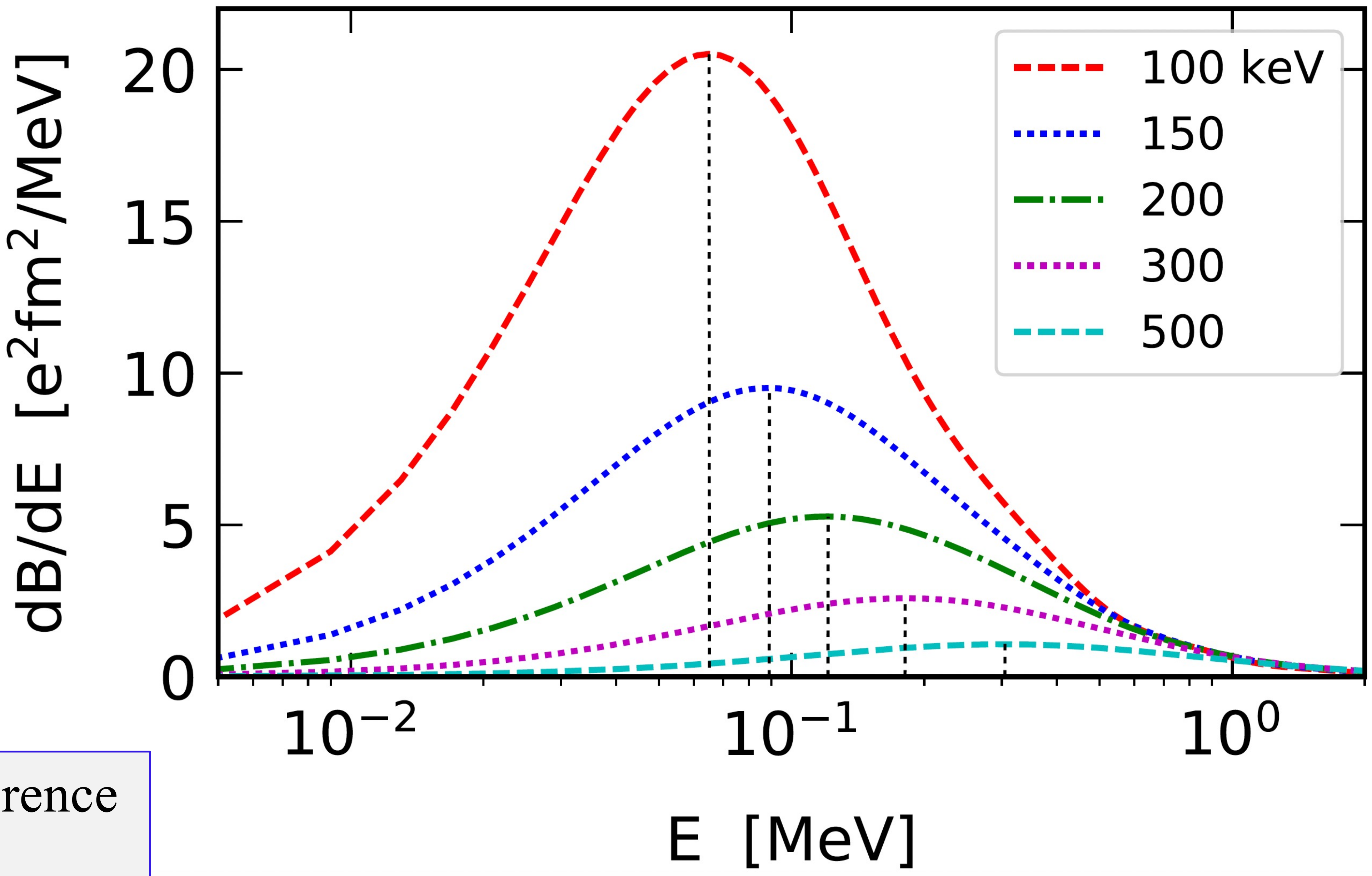

- Excellent agreement < 4% difference
- FSI small

EM response of the hypertriton

1.5 GeV/nuc. ${}^{3}_{\Lambda}$H incident on ^{12}C, ^{120}Sn, ^{208}Pb

B_Λ (keV)	σ_C(C)	σ_C(Sn)	σ_C(Pb)
100	22.9	1457.	3820.
150	14.9	942.	2464.
200	10.7	672.	1755.
300	7.1	438.	1142.
500	4.1	253.	656.

B_Λ (keV)	σ_I(C)	σ_I(Sn)	σ_I(Pb)
100	842.	2516.	3098.
150	824.	2424.	2982.
200	807.	2341.	2876.
300	783.	2220.	2721.
500	749.	2043.	2490.

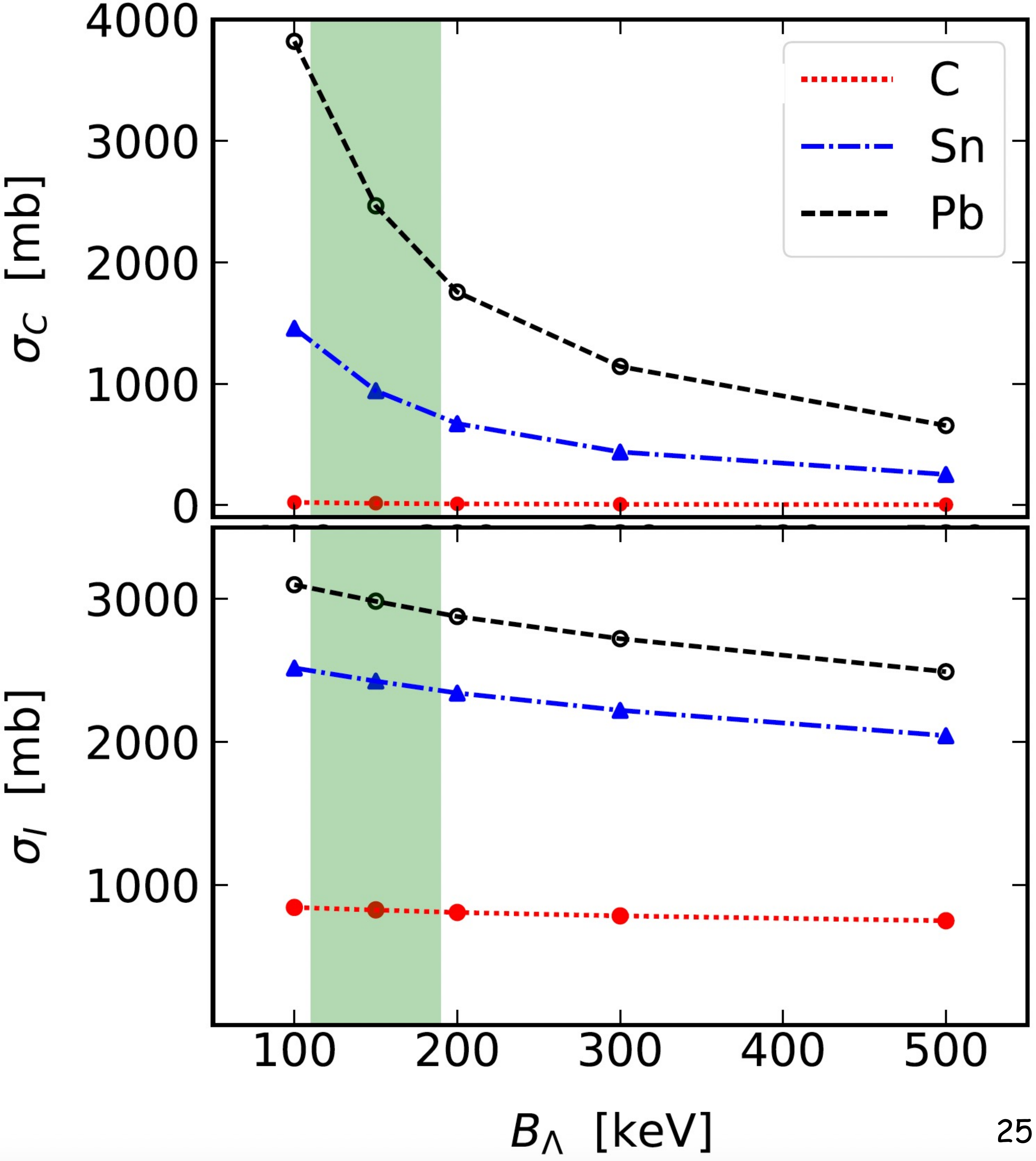

EM response of the hypertriton

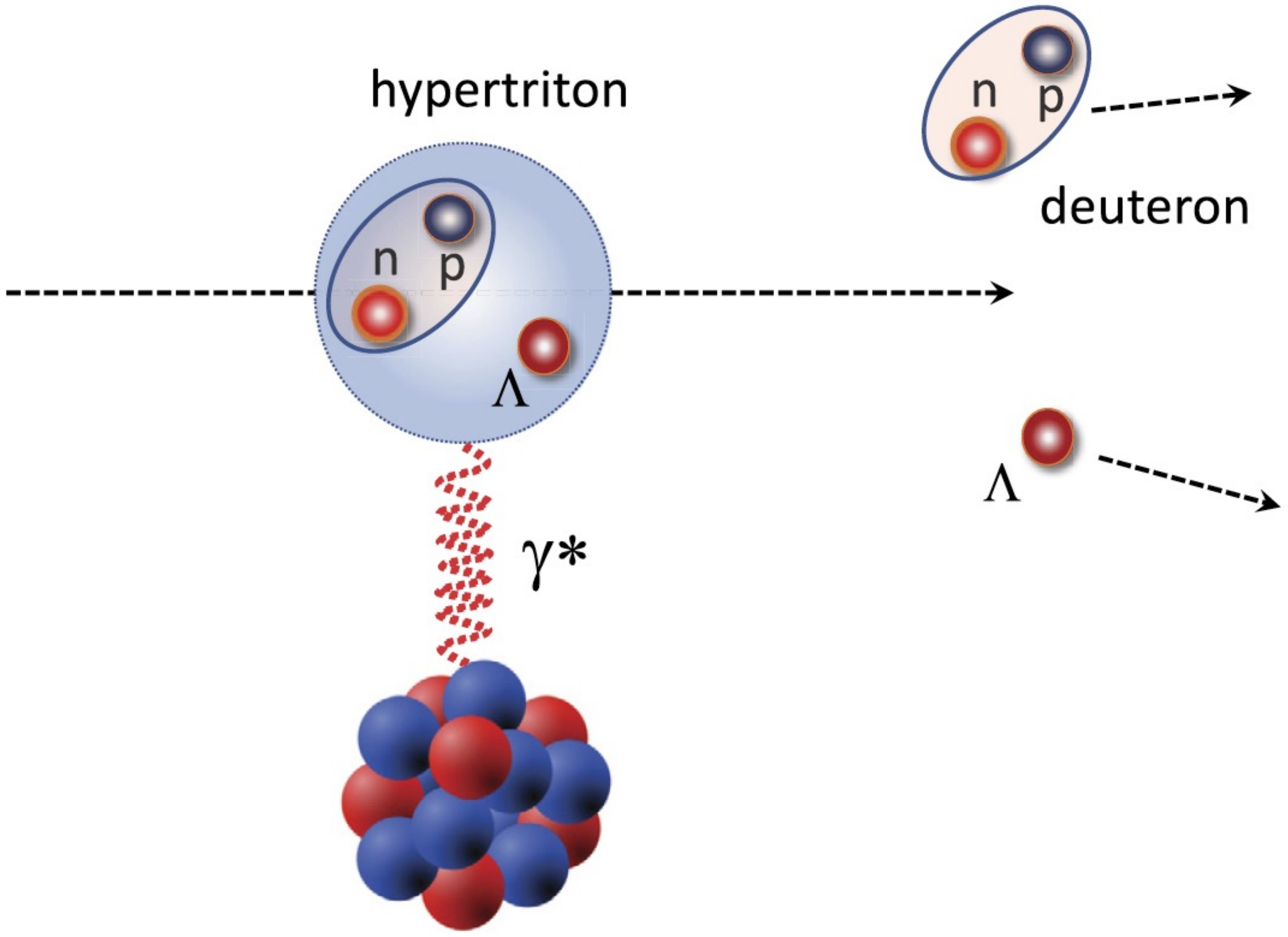

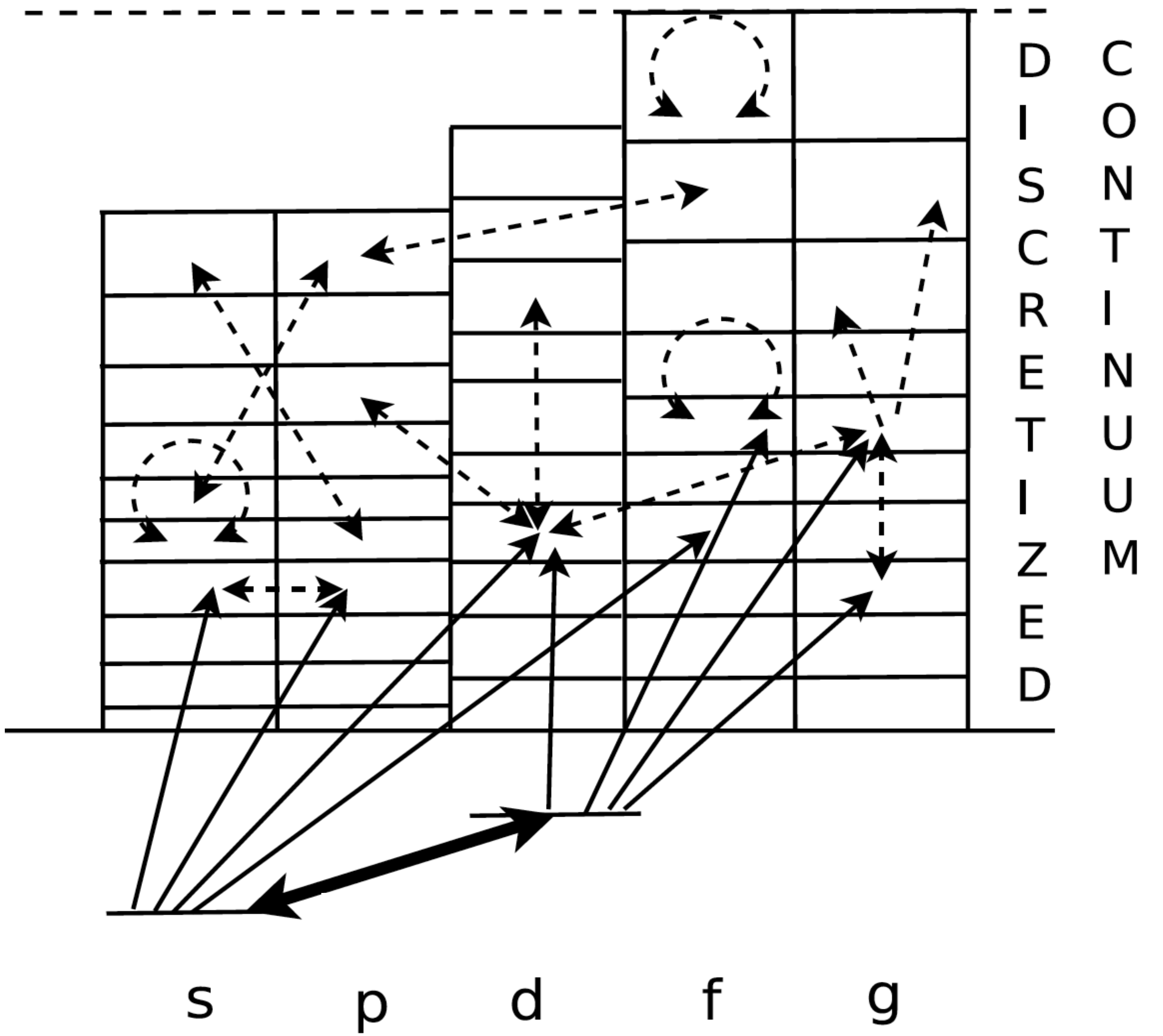

- Basis expansion for intrinsic ϕ
- Eikonal scattering waves
- Nuclear + EM potentials
- Relativity

- Continuum discretization
- Coupled-channels (relativistic CDCC)

Electromagnetic response of loosely bound nuclei

$$i\hbar v \frac{d}{dz} S_c(\mathbf{b}, z) = \sum_{c'} \langle \Phi_c | H_{int}(\mathbf{b}, z) | \Phi_{c'} \rangle S_{c'}(\mathbf{b}, z) \exp\left[i \frac{E_{cc'} z}{\hbar c} \right]$$

$$f_c(\boldsymbol{q}) = -\frac{ik}{2\pi} \int db \exp(i\boldsymbol{q} \cdot \boldsymbol{b}) \left[S_c(\mathbf{b}, z) - \delta_{0c} \right]$$

$$\frac{d\sigma_c}{d\Omega} = \sum_{M_0, M_c} \left| f_c^{(M_c - M_0)}(\theta, E_c) \right|^2$$

$$\left| E_c \right\rangle = \int dE'_c \, \Gamma(E'_c) \left| E'_c \right\rangle$$

$$\Gamma(E_j) = \begin{cases} \dfrac{1}{\Delta E} & \text{if} \quad (j-1)\Delta E < E_c < j\Delta E \\ 0, & \text{otherwise} \end{cases}$$

$H_{int} = H_{EM} = easy$

$H_{int} = H_{nucleus-nucleus}$
$=$ very complicated

Pb (^{8}B,p^{7}Be) at 100 MeV/nucleon

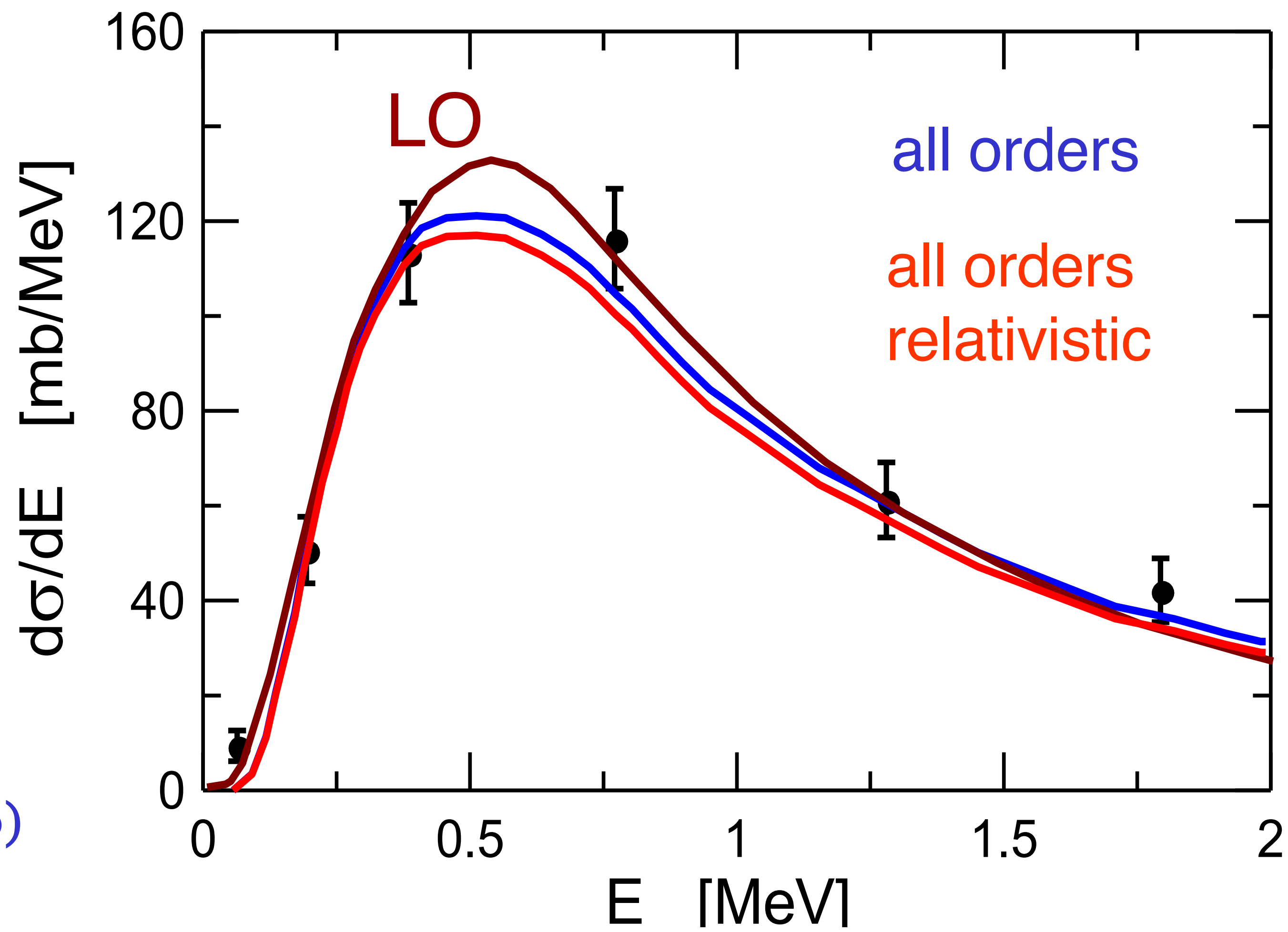

CB, PRL 94, 072701 (2005)

FSI in 3-body models

3-body configurations and FSI widen dB(E1)/dE

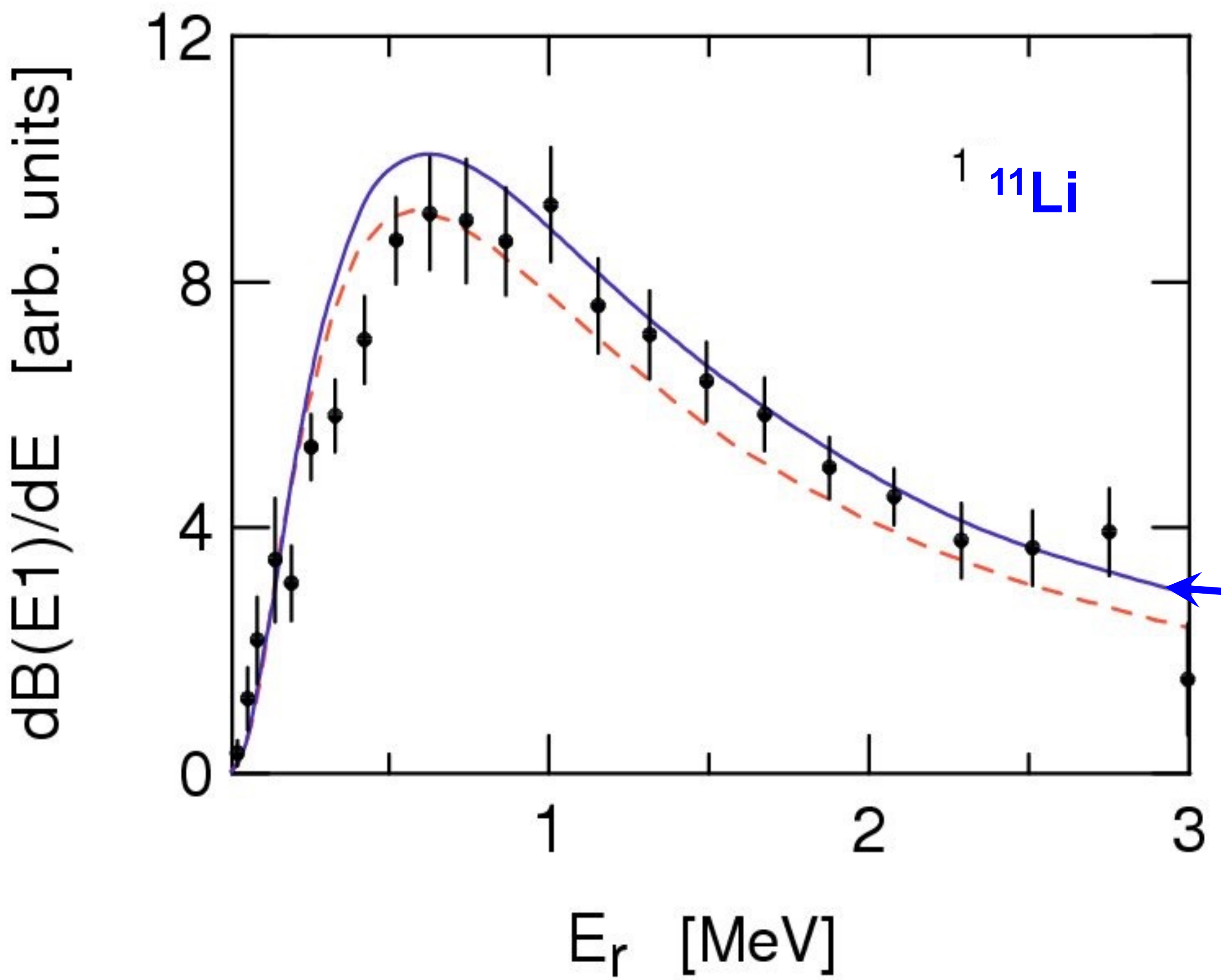

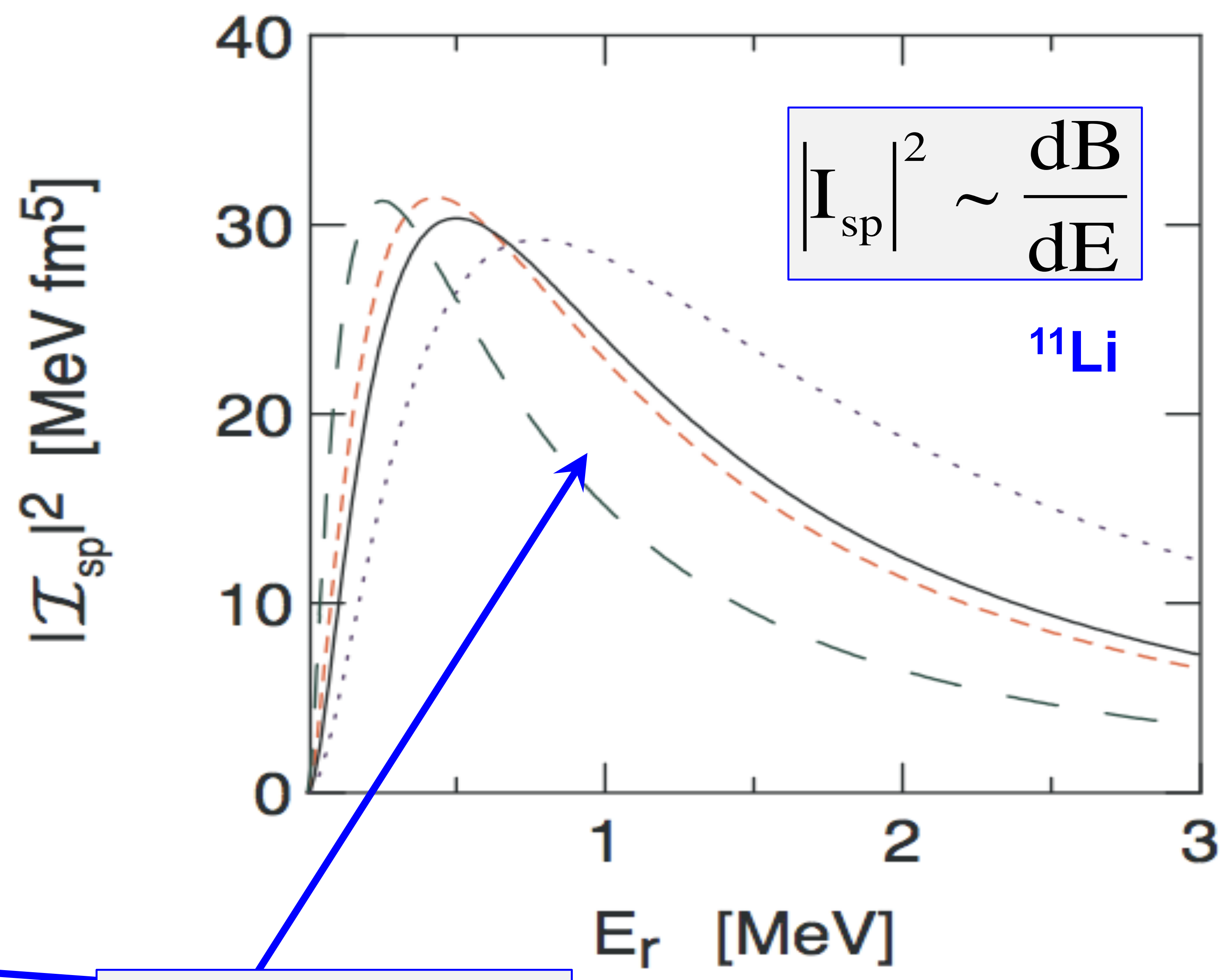

FSI: Different scattering lengths, effective ranges

CB, PRC 75, 024606 (2007)

nn scattering length

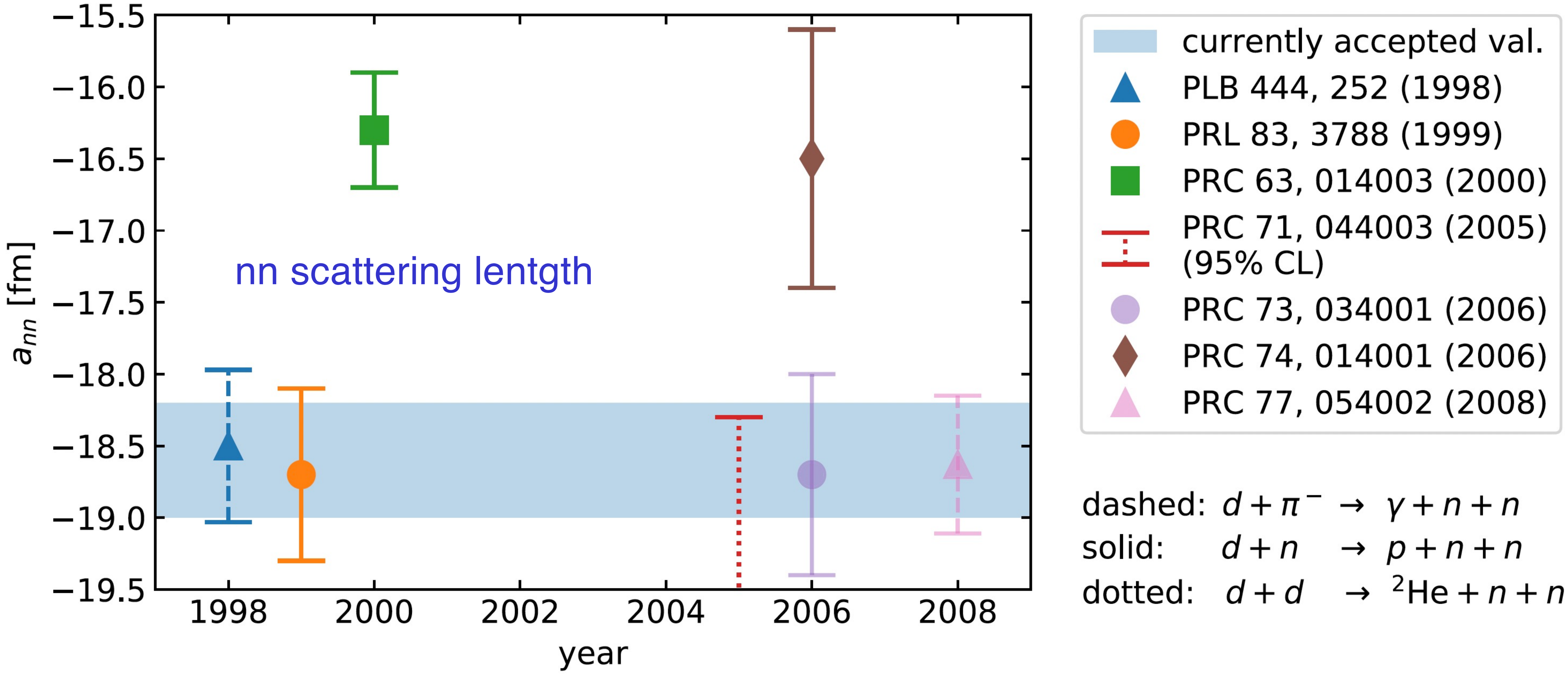

dashed: $d + \pi^- \rightarrow \gamma + n + n$
solid: $d + n \rightarrow p + n + n$
dotted: $d + d \rightarrow {}^2\mathrm{He} + n + n$

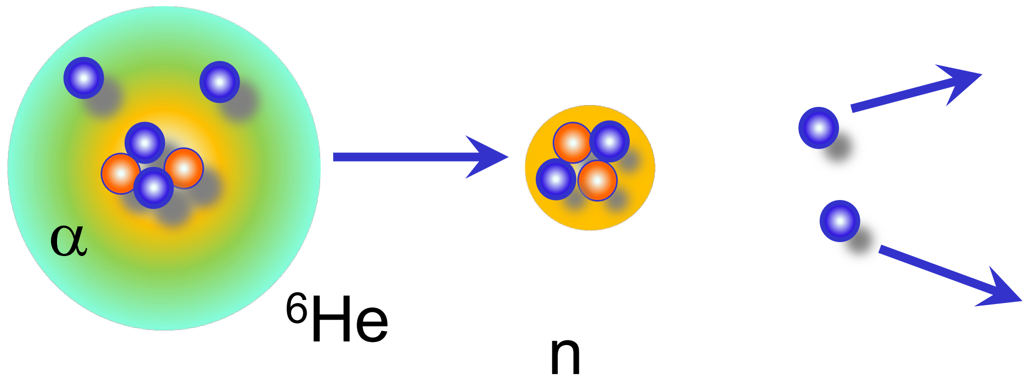

^{6}He(p,pα)nn reaction in inverse kinematics at high energies

Göbel, et al, PRC 104, 024001 (2021)

nn scattering length

Göbel, et al, PRC 104, 024001 (2021)

Halo EFT → nn configuration in ^{6}He → E_{nn} density

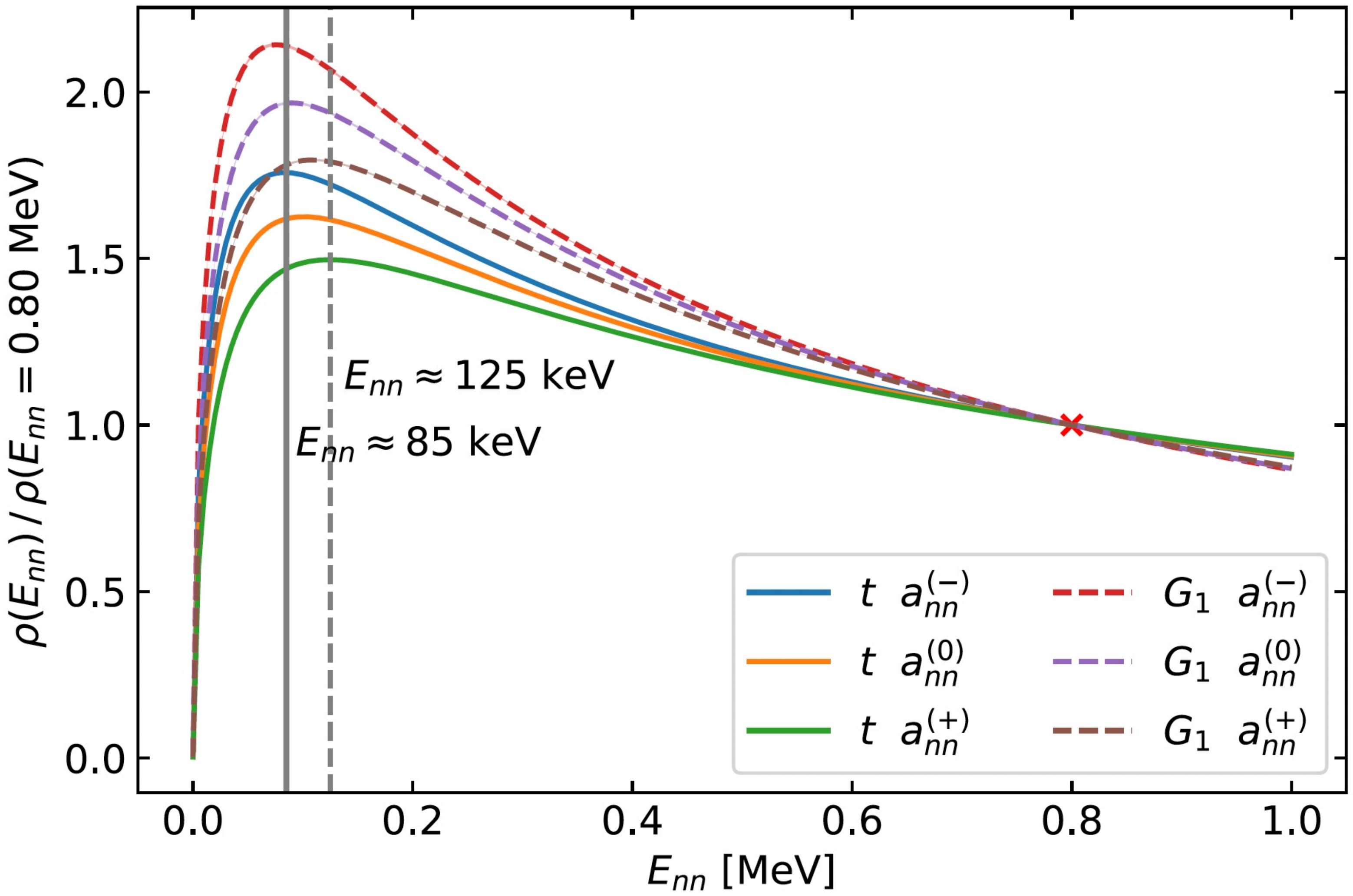

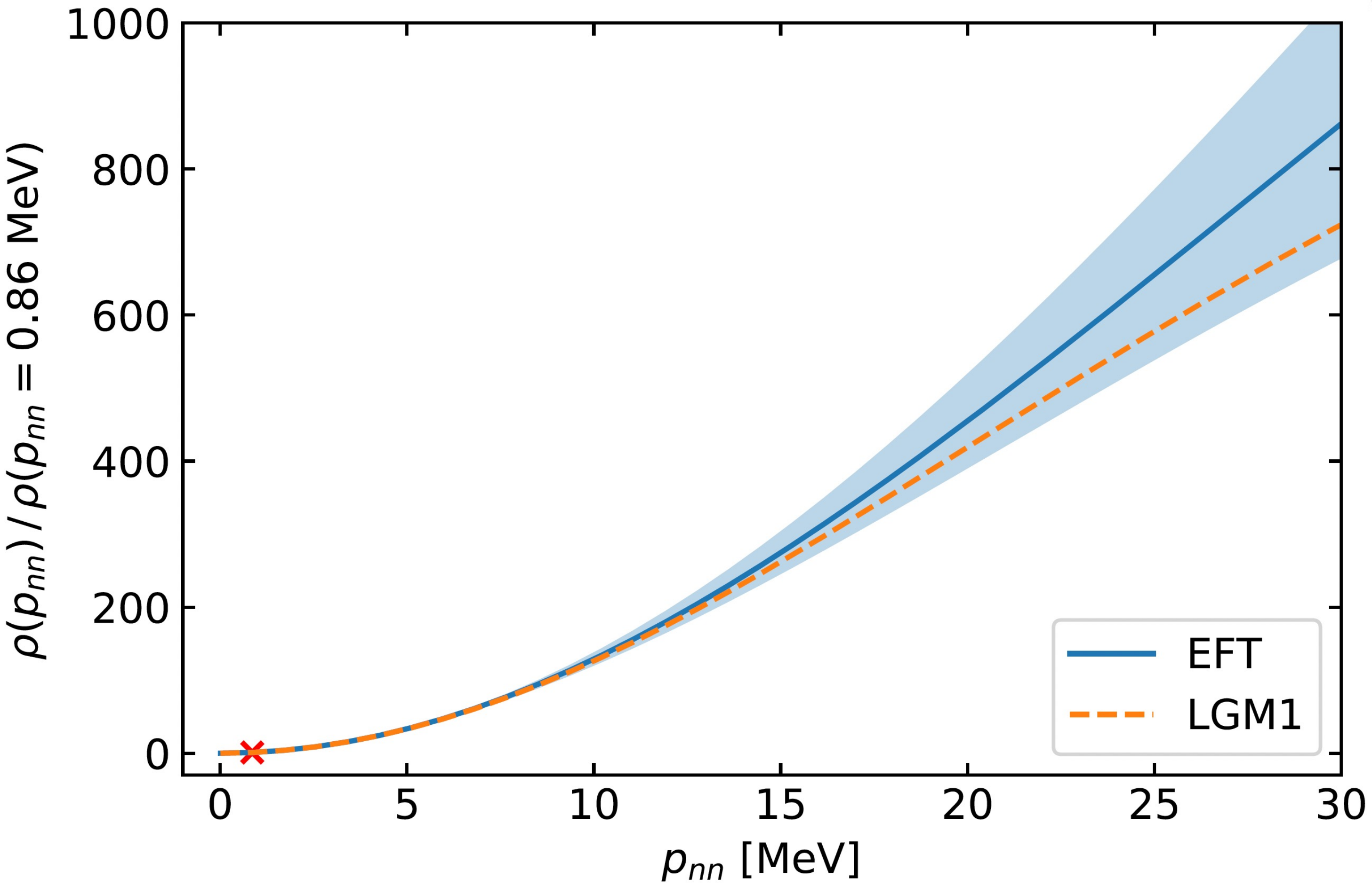

LGM1 = Faddeev calculations with local Gaussian potentials

pp scattering lentgth

v_{NN} charge independence violation: $m_{\pi^\pm} \neq m_{\pi^0}$

v_{NN} charge symmetry violation: $m_{down} \neq m_{up}$

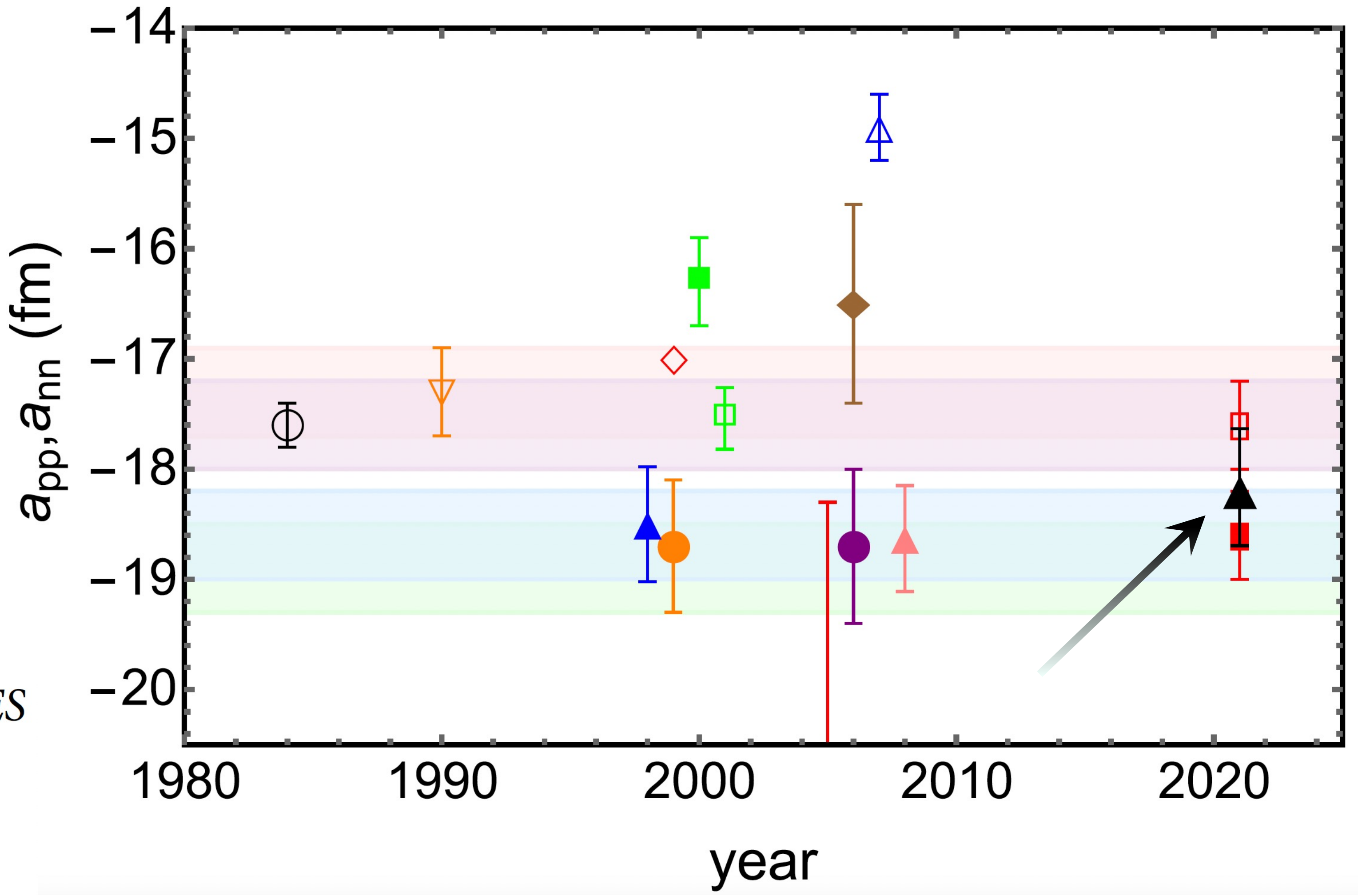

p + d ⟶ p + p + n ➔ p + p scattering

Tumino, et al,
Nature Comm. Phys. 6, 106 (2023)

$$\frac{d^3\sigma}{d\Omega_B d\Omega_b dE_B} = (KF)\cdot|\phi(p_{xs})|^2 \cdot \left[\frac{d^2\sigma_{xA\to bB}}{dE_{c.m.}d\Omega}\right]^{HOES}$$

$$\left(\frac{d\sigma}{d\Omega_{c.m.}}\right)^{HOES} = \frac{1}{4k^2}\left(\left|F(\mathbf{p},\mathbf{k}) - 2T_{CN}(p,k)\right|^2 + 3\left|F(\mathbf{p},\mathbf{k})\right|^2\right)$$

$$F(\mathbf{p},\mathbf{k}) = m_p e^2 e^{-\pi\eta}\Gamma(1+i\eta)(p^2-k^2)^{i\eta} g(\mathbf{p},\mathbf{k})$$

$$g(\mathbf{p},\mathbf{k}) = (\mathbf{p}-\mathbf{k})^{-2(1+i\eta)} \pm (\mathbf{p}+\mathbf{k})^{-2(1+i\eta)}$$

Energy differences between mirror nuclei small as compared to experiment (Nolen-Schiffer anomaly)

pp scattering lentgth

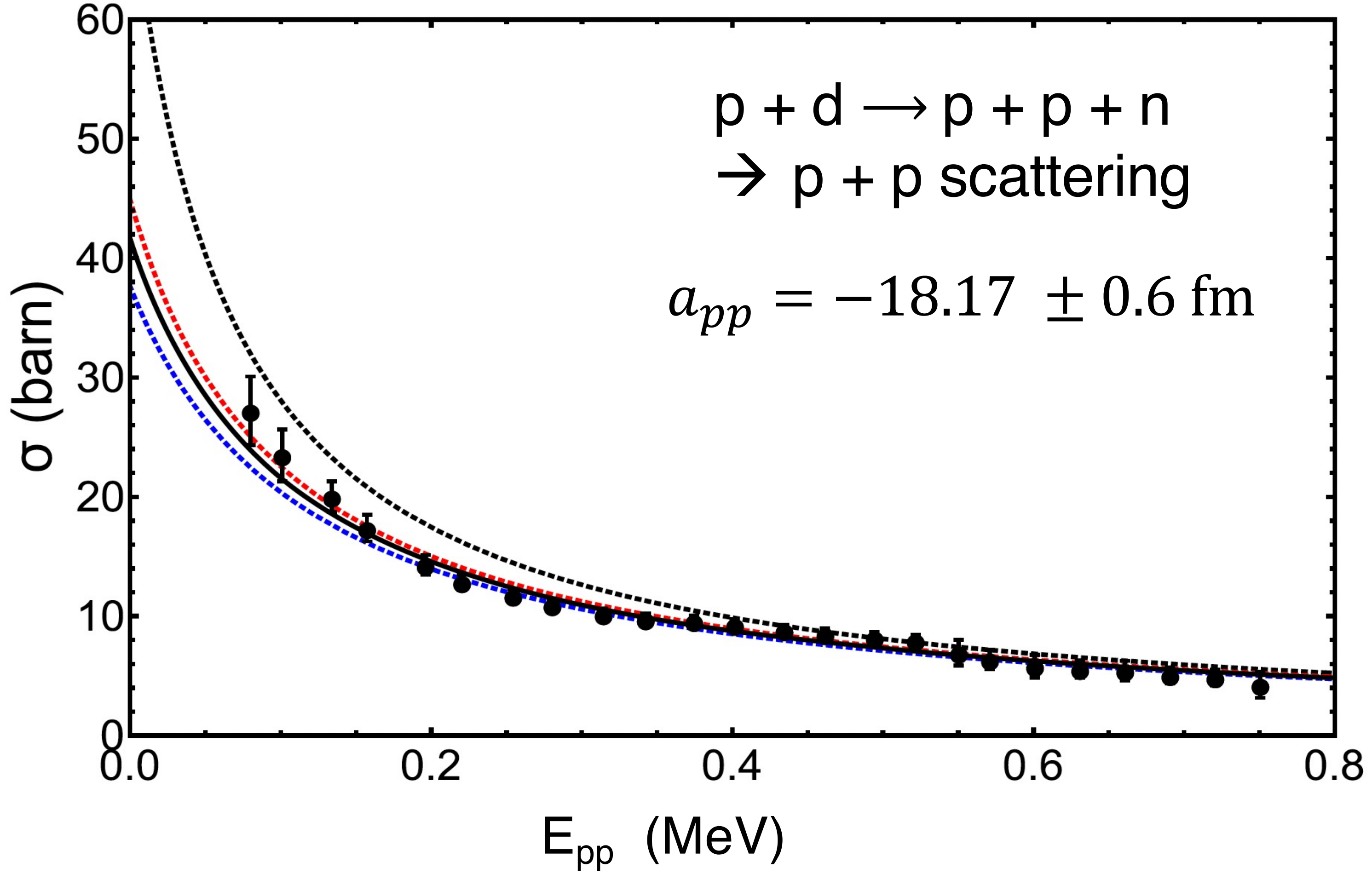

NN s-wave phase shift

$$k \cot \delta = -\frac{1}{a} + \frac{1}{2} r_0 k^2$$

$$\sigma = \frac{4\pi}{\left(\frac{1}{a} - \frac{1}{2} r_0 k^2\right)^2 + k^2}$$

$$V_{NN}(R) = V_0 e^{-\frac{r^2}{r_G^2}} + \frac{e_{NN}^2}{r}$$

disable EM → d from short-range universal window

Table 2 The effect of electromagnetic terms. Low-energy parameters with and without the inclusion of the electromagnetic terms for the two potential models indicated.

	Argonne v_{18}	w/o v^{EM}		Argonne v_{18}	w/o v^{EM}
$^1a_{nn}$(fm)	−18.487	−18.818	$^1a_{pp}$(fm)	−7.806	−17.164
$^1r_{nn}$(fm)	2.840	2.834	$^1r_{pp}$(fm)	2.788	2.865

	Gaussian	w/o v^{EM}		Gaussian	w/o v^{EM}
$^1a_{nn}$(fm)	−18.487	−18.89 ± 0.02	$^1a_{pp}$(fm)	−7.806	−17.19 ± 0.03
$^1r_{nn}$(fm)	2.85 ± 0.07	2.83 ± 0.07	$^1r_{pp}$(fm)	2.77 ± 0.08	2.86 ± 0.08

FSI in light hypernuclei decay

$m_\Lambda = 1115.7$ MeV

$\Gamma = 2.5\times10^{-6}$ eV

$\tau = 263 \pm 2$ ps

$\Lambda \longrightarrow p\pi^-$ (64.1%)

$\Lambda \longrightarrow n\pi^0$(35.7%)

Nonmesonic decays of light hypernuclei is the only tractable way to study ΔS = 1 weak baryon-baryon interaction.

Parker, PRC 76, 035501 (2007)

$$\Gamma_{\text{total}} = \overbrace{\Gamma_{\text{mesonic}}}^{} + \overbrace{\Gamma_{\text{nonmesonic}}}^{}$$
$$= \Gamma_{\pi^-} + \Gamma_{\pi^0} + \Gamma_{\pi^+} \quad \Gamma_p + \Gamma_n + \Gamma_{mb}$$

Γ_{π^-}: $\Lambda \longrightarrow p\pi^-$

Γ_{π^0}: $\Lambda \longrightarrow n\pi^0$

Γ_{π^+}: $p\Lambda \longrightarrow nn\pi^+$

Γ_p: $\Lambda p \longrightarrow np$

Γ_n: $\Lambda n \longrightarrow nn$

Γ_{mb}: $\Lambda NN \longrightarrow NNN$

Two-body nonmesonic decay modes, $\Lambda N \longrightarrow NN$, distinguishable from $\Lambda \longrightarrow \pi N$ because of large decay energy $M_\Lambda - M_N = 176$ MeV. Sensitive to weak interaction couplings (such as $g_{\Lambda N\rho}$ or g_{NNK}) not available to the free Λ decays.

At the quark level:
$$H_{weak} = \frac{G_F}{2} sin\theta_c cos\theta_c [\bar{u}\gamma_\mu(1-\gamma_5)s\bar{d}\gamma^\mu(1-\gamma_5)u]$$

Effective Lagrangian for ΔT=1/2:
$$H_{weak} = -G_F m_\pi^2 \overline{\psi_N}(A_\pi + B_\pi\gamma_5)\phi_\pi \cdot \tau\psi_\Lambda \begin{pmatrix}0\\1\end{pmatrix}$$

Isgur et al, PRL 64, 161 (1990)

$A_\pi = 1.05, \qquad B_\pi = -7.15$

FSI in light hypernuclei decay

CB, Lobato, EPJ A 57, 67 (2021)

Fadeev + approximations

$$\psi_f^{(-)} = \left[1 + \left(E^{(-)} - H_0\right)^{-1} t_{pn}^{\dagger}\right] \chi^{(-)}(\boldsymbol{p}_p)\, \chi^{(-)}(\boldsymbol{p}_n) \psi_{A-2}$$

⇨

$$\Gamma = \frac{2\pi}{\hbar} \sum \int \Big| \Big\langle \chi^{(-)}(\mathbf{p}_p) \chi^{(-)}(\mathbf{p}_n), \Psi_{A-2}(S M_S J_F M_F) \Big| \times \left[1 + t_{pn}\left(\Delta_n - \frac{\hbar^2 \mathbf{P}^2_{pn,cm}}{4 m_N}\right)(\Delta_n - H_0 + i\varepsilon)^{-1}\right] \times V_{weak} \Big| \Psi_A(J_I M_I) \Big\rangle \Big|^2 \delta\left(E_{pn,cm} + E_{pn,rel} - \Delta_n\right) \times \frac{d\mathbf{p}_p}{(2\pi)^3} \frac{d\mathbf{p}_n}{(2\pi)^3} .$$

and similarly for nn

H_0 = kinetic energies of p and n

Δ_n = total energy of three-body system

FSI in light hypernuclei decay

Watson, PR 88,1163 (1952)
Migdal, JETP 1, 2 (1954)

$$F(E_{nN}) = \left| \frac{\psi(k_{nN}, r_{nN})}{\psi^{(0)}(k_{nN}, r_{nN})} \right|^2 = \frac{(1/r_{nN} - 1/a_{nN} + k_{nN}^2 r_{nN}/2)^2}{(-1/a_{nN} + k_{nN}^2 r_{nN}/2)^2 + k_{nN}^2}$$

$$\Gamma = \frac{2\pi}{\hbar} \sum \int \left| \left\langle \chi^{(-)}(\mathbf{p}_p)\chi^{(-)}(\mathbf{p}_n), \Psi_{A-2}(SM_S J_F M_F) \right| \right.$$
$$\times \left[1 + t_{pn} \left(\Delta_n - \frac{\hbar^2 \mathbf{P}_{pn,cm}^2}{4m_N} \right) (\Delta_n - H_0 + i\varepsilon)^{-1} \right]$$
$$\left. \times V_{weak} \left| \Psi_A(J_I M_I) \right\rangle \right|^2 \delta\left(E_{pn,cm} + E_{pn,rel} - \Delta_n\right)$$
$$\times \frac{d\mathbf{p}_p}{(2\pi)^3} \frac{d\mathbf{p}_n}{(2\pi)^3} .$$

FSI in light hypernuclei decay

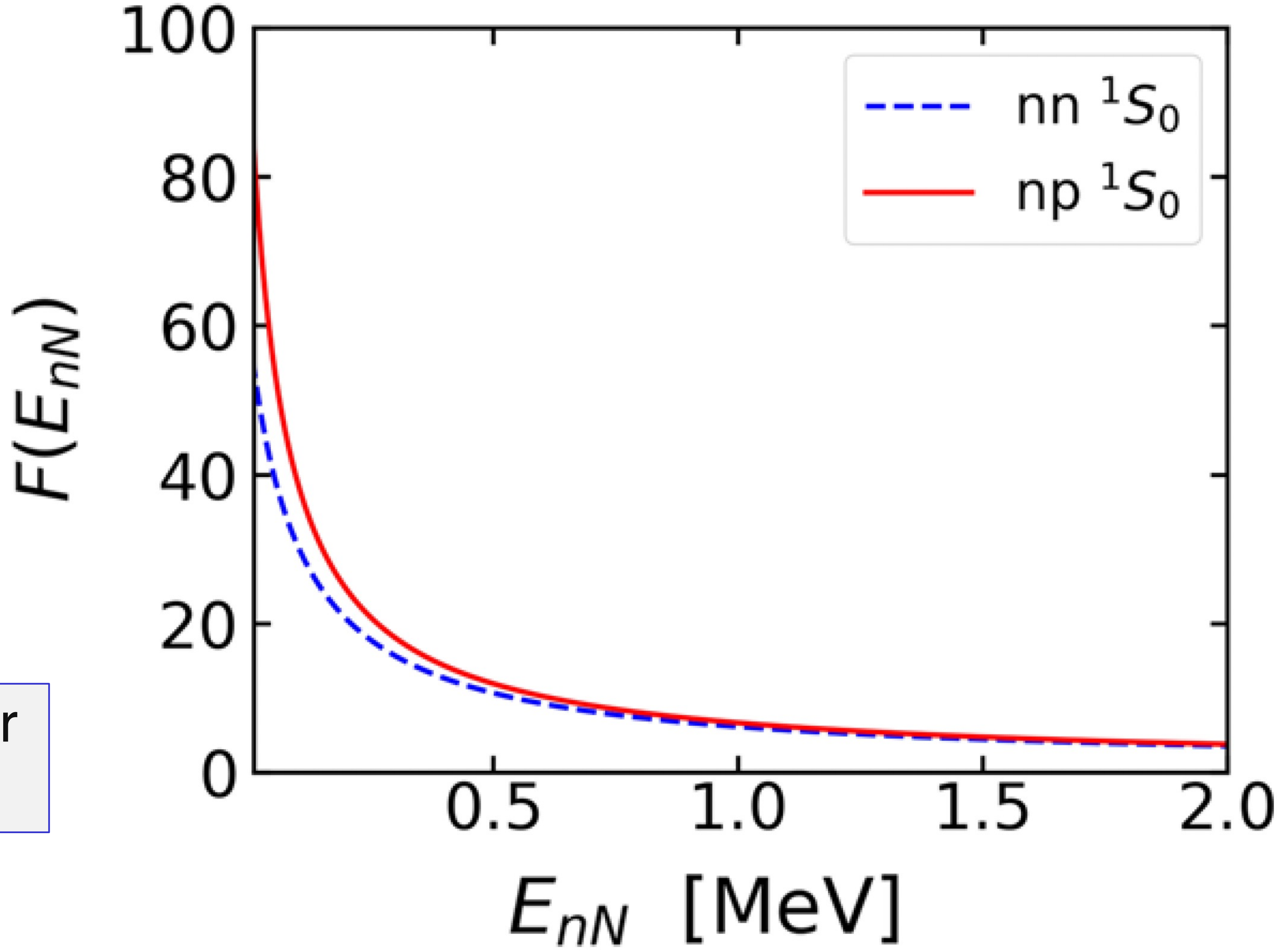

Migdal-Watson enhancement for $^1S_0$ singlet nn and np systems

FSI in light hypernuclei decay

Low energy peak reasonable for the pn channel, while it is quite bad for the nn channel

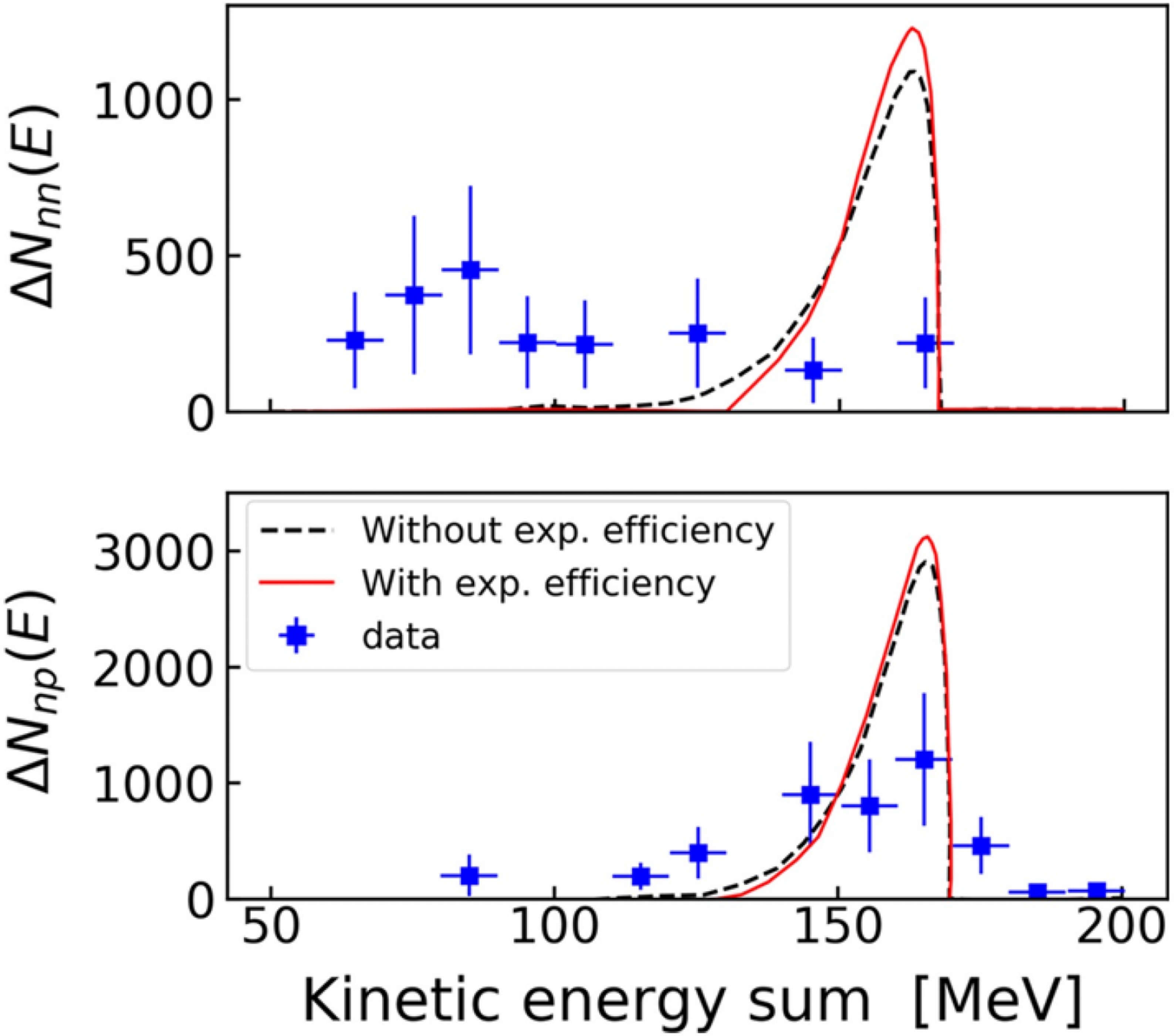

Data:

Parker, PRC 76, 035501 (2007)

FSI in NMWD

Effect of FSI the $^1S_0$ singlet neutron-neutron (nn) and neutron-proton (np) $_\Lambda A$ non-mesonic decay

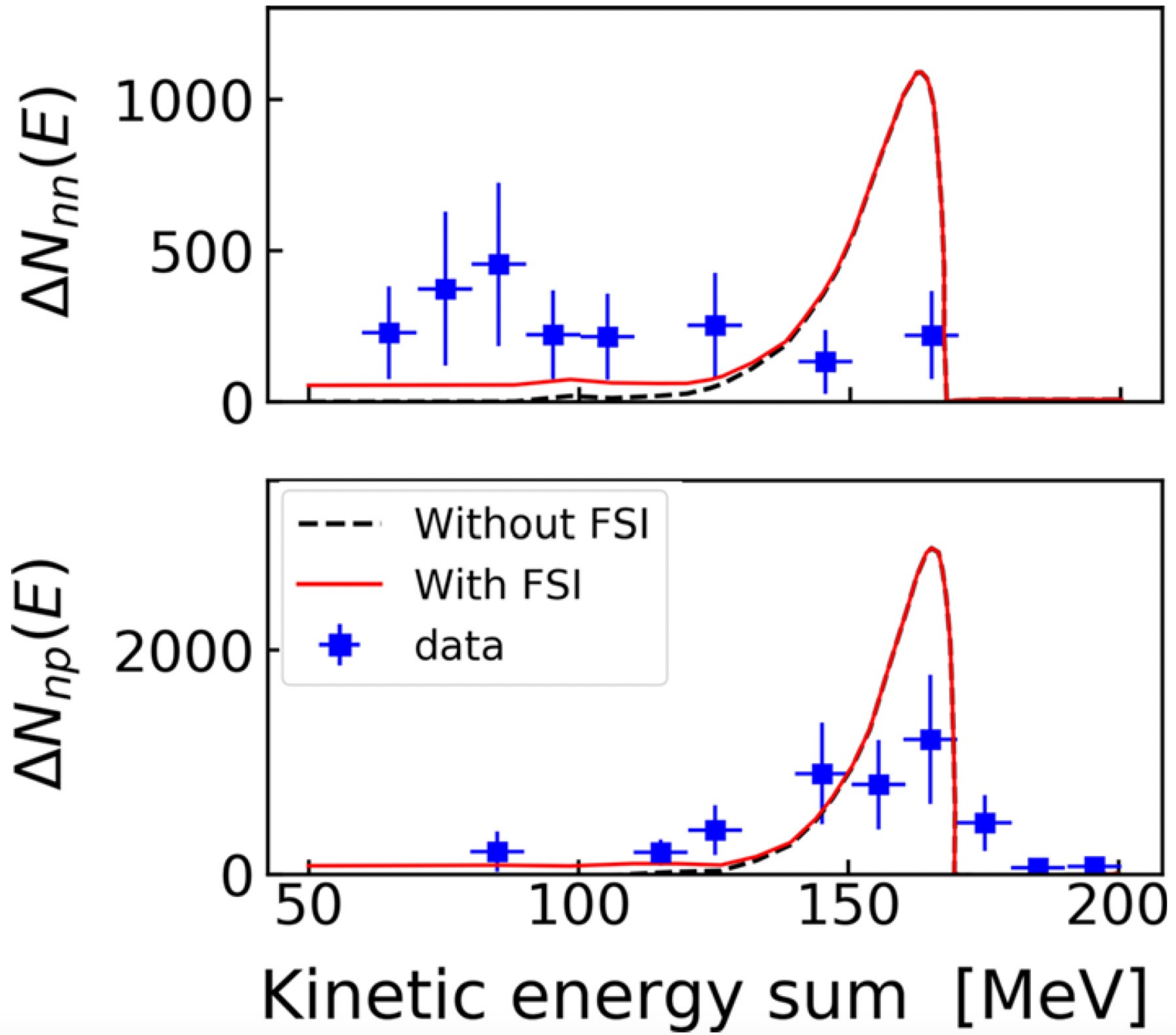

Spin correlations

$$\mathcal{A}(\mathbf{p}_1, \mathbf{r}_1) = \int d^3r\, \chi^{(+)}(\mathbf{p}_1, \mathbf{r}) K(\mathbf{r}, \mathbf{r}_1) \psi_0(\mathbf{r}_1),$$

$K(\mathbf{r}, \mathbf{r}_1)\psi_0(\mathbf{r}_1)$ is the propagator for wavefunction evolution from the source to detector

$\Lambda^{\pm}$ amplitude for singlet (triplet)

$$\Lambda^{(\pm)}(\mathbf{p}_1, \mathbf{p}_2, \mathbf{r}_1, \mathbf{r}_2) = \frac{1}{\sqrt{2}}\Big[\mathcal{A}(\mathbf{p}_1, \mathbf{r}_1)\mathcal{A}(\mathbf{p}_2, \mathbf{r}_2) \pm \mathcal{A}(\mathbf{p}_2, \mathbf{r}_1)\mathcal{A}(\mathbf{p}_1, \mathbf{r}_2)\Big],$$

$$P(\mathbf{p}_1, \mathbf{p}_2) = \int d^3r_1 d^3r_2 \Big|\Big|\Lambda^{(+)}(\mathbf{p}_1, \mathbf{p}_2, \mathbf{r}_1, \mathbf{r}_2)\Big|^2 \pm \mathcal{M}\Lambda^{(-)}(\mathbf{p}_1, \mathbf{p}_2, \mathbf{r}_1, \mathbf{r}_2)\Big|^2\Big|^2\Big],$$

Probability admixture for singlet and triplet states

Correlation function: relative contribution of the singlet and the triplet states in the initial configuration

$$C(\mathbf{p}_1, \mathbf{p}_2) = \frac{P(\mathbf{p}_1, \mathbf{p}_2)}{P(\mathbf{p}_1)P(\mathbf{p}_2)}$$

Spin correlations

Two-body probability density $\mathcal{P}(E_{nn})$
$P(E_{nn}) = \mathcal{P}(E_{nn})\, dE_{nn}$

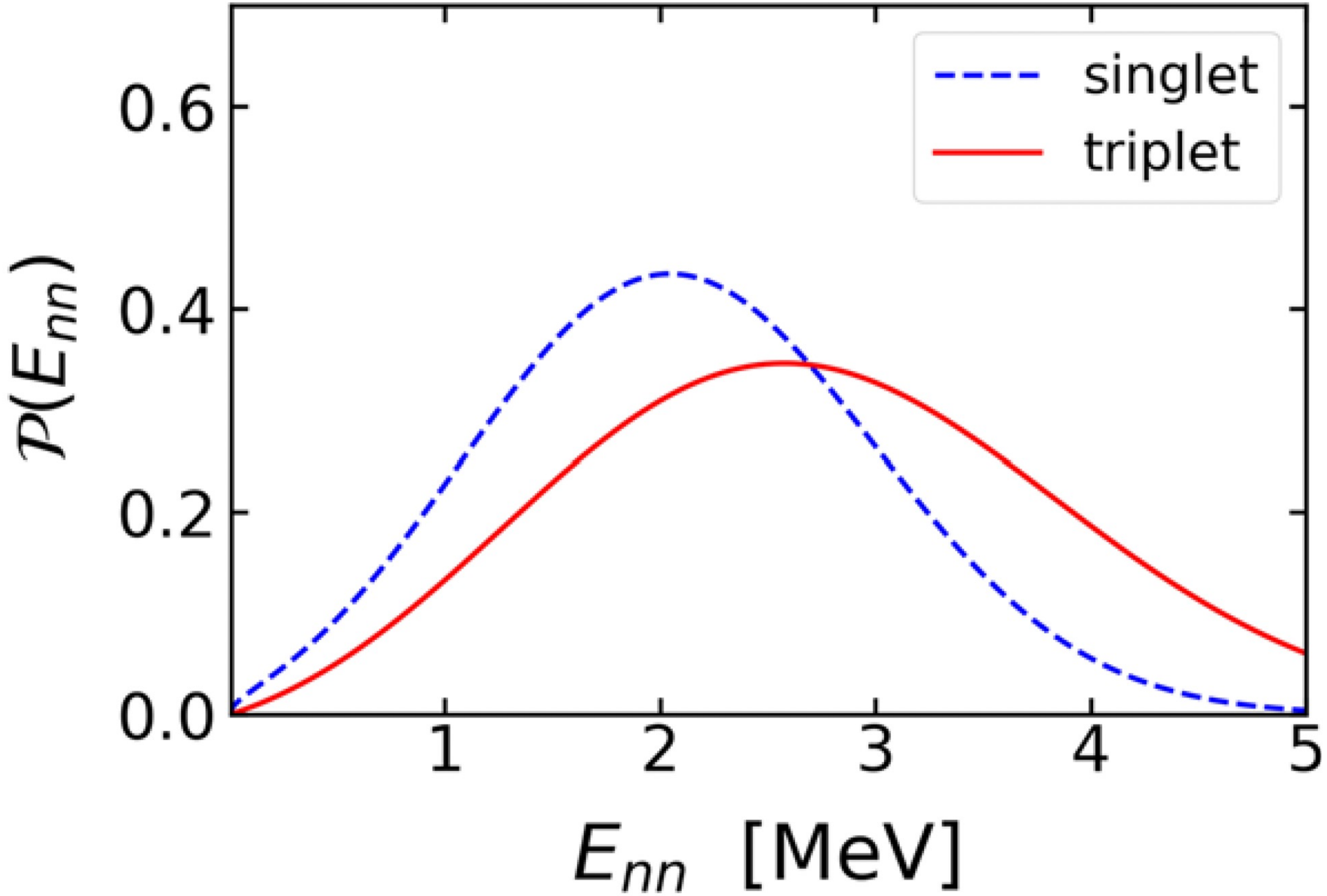

Assuming r_0 = 4 fm for the average initial distance of the nn pair right after the NMWD

⇨

Spin correlations more important than FSI in NMWD

Summary

- Production and fragmentation of hypertriton sensitive to its radius.
- Electromagnetic response of the hypertriton also useful. Maybe will become state-of the art probe in the future.
- Nonmesonic decays of light hypernuclei is the only tractable way to study $\Delta S = 1$ weak baryon-baryon interaction.
- FSI important and can be used to our benefit (scattering lengths, probe of spin correlations, etc).